1972

Design of a near-optimal fluidic operational amplifier

Tahir Mohamed Sheikh
Lehigh University

ABSTRACT

DESIGN OF A NEAR-OPTIMAL FLUIDIC OPERATIONAL AMPLIFIER

Tahir Mohamed Sheikh

Two near-optimal designs of a fluidic operational amplifier using commercially available cascaded proportional amplifiers are presented. The characteristics of the five-stage proportional amplifier were experimentally determined in a previous study. Both designs utilize forward path compensation instead of the conventional feedback path compensation and have a good response for low and moderate frequencies. The first or basic design is virtually optimal assuming on a particularly simple model of the five-stage amplifier. The second or modified design is virtually optimal for a model which better represents the measured behavior, but at frequencies above which the data was taken is expected to be inferior.

The basic operational amplifier was tested for static gain characteristics and frequency response. The results are of qualitative usefulness only due to fabrication problems with the input and feedback resistances. Magnitudes and phase lag of the closed loop gain is also predicted up to a frequency of 1000 Hz. and compared with the experiment. Design details of the modified model are presented but the design was not actually fabricated.

DEFINITIONS

AEC	- Atomic Energy Commission
AFOSR	- Air Force Office of Scientific Research
AISC	- American Institute of Steel Construction, Inc.
AISI	- American Iron and Steel Institute
ARO-D	- Army Research Office-Durham
EPA	- Environmental Protection Agency
HEW	- U. S. Department of Health, Education and Welfare
IDRES	- Institute for the Development of Riverine and Estuarine Systems
NADC	- Naval Air Development Center
NASA	- National Aeronautics and Space Administration
NEH	- National Endowment for the Humanities
NIMH	- National Endowment for the Humanities
NOAA	- National Oceanic and Atmospheric Administration
NPIRI	- National Printing Ink Research Institute
NSF	- National Science Foundation
ONR	- Office of Naval Research
PennDOT	- Pennsylvania Department of Transportation
PHS	- Public Health Service
PSEF	- Pennsylvania Science and Engineering Foundation
RCRC	- Reinforced Concrete Research Council
W-PAFB	- Wright-Patterson Air Force Base

DESIGN OF A NEAR-OPTIMAL FLUIDIC OPERATIONAL AMPLIFIER

by

Tahir Mohamed Sheikh

A Thesis
Presented to the Graduate Committee
of Lehigh University
in Candidacy for the Degree of
Master of Science
in
The Department of Mechanical Engineering and Mechanics

Lehigh University

1972

This thesis is accepted and approved in partial fulfillment of the requirements for the degree of Master of Science.

Aug 3, 1972
(date)

James T. Brown
Professor in Charge

E. Dumbleton for EPB
Chairman of Department

ACKNOWLEDGEMENT

Throughout this study the author received most valuable guidance from his teacher and thesis advisor, Professor Forbes T. Brown to whom the author wishes to express his gratitude.

The work was supported by the Office of Naval Research under Contract No. N00014-69-A-0417.

TABLE OF CONTENTS

LIST OF FIGURES

ABSTRACT

Two near-optimal designs of a fluidic operational amplifier using a commercially available cascaded proportional amplifier are presented. The characteristics of the five-stage proportional amplifier were experimentally determined in a previous study. Both designs utilize forward path compensation instead of the conventional feedback path compensation and have a good response for low and moderate frequencies. The first or basic design is virtually optimal assuming on a particularly simple model of the five-stage amplifier. The second or modified design is virtually optimal for a model which better represents the measured behaviour, but at frequencies above which the data was taken is expected to be inferior.

The basic operational amplifier was tested for static gain characteristics and frequency response. The results are of qualitative usefulness only due to fabrication problems with the input and feedback resistances. Magnitudes and phase lag of the closed loop gain is also predicted up to a frequency of 1000 Hz. and compared with the experiment. Design details of the modified model are presented but the design was not actually fabricated.

NOMENCLATURE

A	Area of cross-section
C	Compliance
C_c	Compliance of volume at control port
C_o	Compliance of volume at output port
C_3, C_4	Partial compliances of tube in load Y_{al}
d	Diameter
E	Energy
F	Correction factor for transfer characteristics of proportional amplifier
f	Fundamental frequency (Hz)
f_n	Natural frequency (Hz)
g	Gain
I	Inertance
I_c	Inertance of hypodermic tubes at control ports
I_o	Inertance of hypodermic tubes at output ports
I_4	Inertance of tube in load Y_{al}
m	Mass
P	Pressure
P_i	Inside pressure
P_o	Outside pressure
P_{ic}	Inside pressure at control ports
P_{io}	Outside pressure at output ports
$(Pi)_a$	Actual inside pressure

$(Pi)_{id}$	Ideal inside pressure
Q	Flow rate
Q_a	Actual flow rate
Q_{id}	Ideal flow rate
R	Resistance
R_c	Resistance of hypodermic tubes at control ports
R_o	Resistance of hypodermic tubes at output ports
R_1, R_1'	Resistance from input to summing function
R_2	Defined separately for conventional and basic designs (see figures 4 and 6)
R_3	Defined separately for conventional and basic designs (see figures 4 and 6)
R_4	Feedback Resistance
s	Laplace variable d/dt
T	Delay time
t	Time, thickness
V	Volume
v	Velocity
w	Width
Y	Admittance
Y_a	Actual load admittance
Y_{a1}	Actual load admittance used in determining transfer characteristic
Y_{a2}	A second actual load not containing a volume
Y_o	Output admittance of operational amplifier

Y_i	Input admittance of operational amplifier
Z	Impedance
Z_o	Output impedance of amplifier

Greek Symbols

τ	Time constant
ω	Fundamental frequency (rad/sec)
ω_n	Natural frequency (rad/sec)
ζ	Damping coefficient
ρ	Density of air
μ	Dynamic viscosity of air
ν	Kinematic viscosity of air

1. INTRODUCTION

A proportional amplifier is a constant flow device in which control inputs proportionally divert fluid from one port to another and can be built as a pressure amplifier, flow amplifier, or power amplifier depending on the operational needs. Cascaded stages of such elements are capable of exceedingly high pressure gains and are used with feedback to produce operational amplifiers, summing circuits, integrators, etc. The virtue of this feedback design is excellent linearity and saturation with a relatively high output admittance and gains which are virtually independent of supply pressure for wide variations.

The usual approach is to sharply reduce the amplitude of the feedback signals at high frequencies by inserting large volumes in the feedback path as shown in figure 4. The response of the pressure using this approach is good for very small input amplitudes and slow input of change. For other than these conditions, however, the amplifier saturates and the results do not hold.

The feedback volumes also prevent the linearized behaviour from approaching the idealized optimum. The most significant conclusion is that all rate-limiting effects can be virtually eliminated by removing all dynamic elements from the feedback path and instead placing them in the forward path. This is the apporach used in the design

of the Basic Operational Amplifier (see figure 6). The only dynamic element is a blocked resonance tube placed in the forward path. To understand this consider a step input to the operational amplifier. The step is drastically reduced by the shunt resonator tube, creating a wave in the tube which heads towards the blocked end. The attenuation is such that the output of the cascaded amplifier is a delayed step of the proper steady-state amplitude (no transient saturation!) since the proportional amplifier is ideally a constant gain with time delay T. This change in output pressure is transmitted around the feedback loop to the resonator tube arriving just as the initial wave returns from the blocked end where it was reflected. The two step changes then precisely cancel one another and no further changes occur. Thus the overall response is the theoretical ideal with no saturation effect. (Except of course when steady-state involves saturation.)

The characteristics needed for the optimization are the input and output impedances of the gain block and its transfer characteristics which include gain and phase information. A General Electric model AM-12 five-stage proportional fluidic amplifier advertized by G. E. to have a blocked gain of 2300 and a phase lag of 0.2 degrees per Hz is used in the design of the operational amplifier. The

characteristics as measured by J. Boparai[†] are shown in figures 13 to 16, 19 and 20.

As seen in figure 26, the phase lag of the loop gain of the cascaded amplifier does not increase linearly with frequency. Furthermore the prospects for a good response of this design at quite high frequency is poor. These facts combine to suggest a modified compensator which is nearly optimum. This modified design results from a second transfer function representation of the cascaded amplifier.

Experimental tests were conducted with the Basic Operational Amplifier. Static gain measurements and frequency response data were taken. Unfortunately, phase information could not be secured due to excessive noise, and the magnitude data was seriously marred by erroneous values of the input and feedback resistances, which varied severely with different applications of vacuum grease and different clamping arrangements. Magnitude and phase of the closed-loop gain are predicted for the Basic Design of the Operational Amplifier.

[†]Boparai, J. S., "Measurement of Dynamic Characteristics of Five-Stage Proportional Fluidic Amplifier", M. S. Thesis Lehigh University, Bethlehem, Pennsylvania, 1972.

2. CHARACTERISTICS OF THE CASCADE AMPLIFIER

2.1 Introduction

The dynamic characteristics of the five-stage proportional amplifier (General Electric model AM-12) were experimentally measured at the Lehigh University laboratory by Boparai. The circuitry as used in the experimental determination is shown in figure 1(b). Calibrated flow resistances (bundles of hypodermic tubes) were placed at two control and output ports and pressure measurements were made at the two ends.

In the evaluation of the input and output admittances Boparai neglected the effects of the inertance of the hypodermic tubes and the compliance of the volumes at their two ends. In this chapter a correction is derived. To do this the time constants are evaluated from first principles and then compared with experiment. The output admittance is also roughly corrected for cross-talk and for operating conditions for which the operational amplifier is to be designed.

2.2 Determination of the Time Constants and Self-Admittances

The approximate electrical analogy of the experimental apparatus used in determining the characteristics is shown

in figure 1(b) and its associated bond graph in figure 2. From the bond graph one obtains

$$YR = \frac{1}{1 + \tau_1 s}\left[\frac{P_o}{P_i} - 1\right] - \tau_2 s \qquad (2\text{-}1)$$

where R is the resistance of the hypodermic tubes

$$\tau_1 = \frac{I}{R}$$

$$\tau_2 = RC$$

This equation is in effect a correction on the one used by Boparai which is

$$YR = \frac{P_o}{P_i} - 1 \qquad (2\text{-}2)$$

The inertance I of the hypodermic tubes can be obtained from the energy equation

$$E = \int \frac{v^2}{2}\, dm = \frac{1}{2} IQ^2$$

$$I = \frac{4}{3}\frac{\rho L}{A} = \frac{4\rho L}{3n\pi r^2} \qquad (2\text{-}3)$$

where n is the number of hypodermic tubes (196), and the factor of $\frac{4}{3}$ results from assuming a parabolic velocity profile across the tubes. The value of the compliance is given by $C = \frac{V}{P}$ for isothermal flow (2-4a)

$$C = \frac{V}{\gamma P} \text{ for adiabatic flow} \qquad (2\text{-}4b)$$

where P is the mean absolute pressure and V is the volume. Isothermal flow was assumed in actual calculations. The time constants for both the control and output sides at zero flow can be obtained by using the value of the resistors at zero flow from their calibrations.

When the external circuitry from either end is isolated from the amplifier by blocking the connecting port (Y = 0), equation (2-1) gives

$$\frac{P_o}{P_i} = 1 + \tau_2^\circ s + \tau_1^\circ \tau_2^\circ s^2 \qquad (2\text{-}5)$$

Figures 17 and 18 show P_o/P_i using time constants at zero flow evaluated by using the values of inertance from eq. (2-3) and compliance from eq. (2-4). These values of P_o/P_i are compared with experiment which consisted of measuring P_o and P_i on both the control and the output circuits at various frequencies and values of τ_1 and τ_2 were selected by trial and error to best suit the data. The time constants with flow can be obtained from

$$\tau_1 = \tau_1^\circ \frac{R^\circ}{R}$$

$$\tau_2 = \tau_2^\circ \frac{R}{R^\circ}$$

where τ_1° and R° are the values at no flow conditions.

The experiment for the output admittance was performed for one-sided excitation only (not push-pull) and is shifted to the right to correct approximately for 17% cross-talk and for the no flow conditions. The admittance can then be evaluated using eq. (2-1) employing the experimentally determined time constants and is shown in figure 19. A similar correction using the same equation is applied on the input admittance of figure 20 to obtain the modified input admittance shown in figure 21.

2.3 The Transfer Characteristics

The experiments for the magnitudes of the pressure ratio P_{io}/P_{ic} were run again at the same frequencies and is shown in figure 24. This would have been the transfer characteristics if the load had been ideal, but the actual load as seen by the output ports comprises of variables more than just a resistor and is shown in figure 3(c). From the bond graph the impedance of the load as seen from the left is

$$\frac{1}{Y_{al}} = \frac{1}{\Delta C_o s}\left[1 + \frac{R_o}{I_o s} + \frac{1}{I_o C_3 s^2} + \frac{1}{I_4 C_3 s^2} + \frac{1}{I_4 C_4 s^2} + \frac{R_o}{I_o I_4 C_3 s^3} + \frac{R_o}{I_o I_4 C_4 s^3} + \frac{1}{I_o I_4 C_3 C_4 s^4}\right] \tag{2-6}$$

where

$$\Delta = 1 + \frac{R_o}{I_o s} + \frac{1}{I_o C_o s^2} + \frac{1}{I_o C_3 s^2} + \frac{1}{I_4 C_3 s^2} + \frac{1}{I_4 C_4 s^2}$$

$$+ \frac{R_o}{I_o I_4 C_3 s^3} + \frac{R_o}{I_o I_4 C_4 s^3} + \frac{1}{I_o I_4 C_o C_3 s^4} + \frac{1}{I_o I_4 C_o C_4 s^4}$$

$$+ \frac{1}{I_o I_4 C_3 C_4 s^4}$$

The variables C_o and I_o have been evaluated from the experimentally determined time constants, and C_3, C_4 and I_3 from equations (2-3) and (2-4a). The actual load is plotted in figure 22. For any load Y_a (see figs. 3(a) and (b)).

$$Q_a = Y_a (Pi)_a$$

$$Q_{id} = Y_{id} (Pi)_{id}$$

$$(Pi)_{id} = (Pi)_a + P_f$$

$$Q_{id} = Q_a - Q_f$$

where $Q_f = \frac{P_f}{Z_o}$

From the above one obtains

$$\frac{(Pi)_{id}}{(Pi)_a} = \frac{Y_a + 1/Z_o}{Y_{id} + 1/Z_o}$$

This experiment was performed under blocked conditions

$$Y_{id} = 0$$

$$\frac{(Pi)_{id}}{(Pi)_a} = 1 + Y_a Z_o$$

$$F = 1 + Y_a Z_o \qquad (2\text{-}7)$$

where F is the correction factor to be applied to the transfer characteristics of figure 24. The correction factor has been plotted in figure 23 for frequencies at which the data was taken. The corrected transfer characteristics are shown in figure 25.

As a check the magnitude ratio of inside pressures at the output port to that at the control side were measured for another load Y_{a2} shown in figure 3(d) from which one obtains

$$Y_{a2} = C_o s \left[1 + \frac{1}{1 + \tau_2 s + \tau_1 \tau_2 s^2}\right] \qquad (2\text{-}8)$$

Y_{a2} is plotted alongside Y_{a1} in figure 22 and the transfer characteristics have been corrected for using the correction factor F evaluated with Y_{a2} from eq. (2-7). Here only the magnitudes have been checked and the same corrected phase as obtained with Y_{a1} is used. The magnitude information is seen to agree fairly well.

3. DESIGN OF THE OPERATIONAL AMPLIFIER

3.1 Conventional Design of Operational Amplifiers

The usual design of a fluidic operational amplifier in figure 4 employs volumes in the feedback path. These volumes serve to attenuate the feedback signals at high frequencies which is essential to achieving stability of the circuit. Let us assume the nominal representation for the fluidic amplifier, which is a constant gain g with time delay T and a real constant input admittance Y_i and output impedance Z_o. Then the overall pressure characteristic is

$$\frac{P_o}{P_i} = -\frac{R_2 + R_3}{R_1} \frac{\left(1 + \frac{R_2 R_3 Cs}{R_2+R_3}\right) - \frac{Z_o}{(R_2+R_3)ge^{-Ts}}}{1 + \frac{(\tau s+1)a}{ge^{-Ts}}} \qquad (3\text{-}1)$$

$$\tau a = \left(\frac{1}{R_1} + \frac{1}{R_1'} + Y_i\right)R_2C(R_3+Z_o+R_3Z_oY_o) + (R_3+R_3Z_oY_o+Z_o)C$$

$$a = 1 + \left(\frac{1}{R_1} + \frac{1}{R_1'} + Y_i\right)(R_2+R_3+Z_o)+Z_oY_o\left[1+\left(\frac{1}{R_1}+\frac{1}{R_1'}+Y_i\right)\right.$$

$$\left.(R_2+R_3)\right]$$

The right-hand term in the numerator of eq. (3-1) represents the direct pressure transmission through the feedback

path and usually is quite negligible. To simplify our considerations, let us set $R_1 = R_1'$ and $Y_o = 0$ and define $R = R_2 + R_3$. For stability it is necessary that

$$a\tau > gT$$

To keep as high a frequency response as practical we employ the value

$$a\tau = (1 + \frac{2R_2}{R_1} + Y_i R_2)(R - R_2 + Z_o)C = \frac{gT}{2} \qquad (3\text{-}2)$$

Now eq. (3-1) becomes

$$\frac{P_o}{P_i} \simeq - \frac{R}{R_1} \frac{1 + \frac{R - R_2}{R} R_2 Cs}{1 + \frac{Ts}{2e^{-Ts}}} \qquad (3\text{-}3)$$

which shows the desired behavior $\frac{P_o}{P_i} \simeq - \frac{R}{R_1}$ as $s \to 0$

With the same approximations and values of the parameters the flow emanating from the five-stage amplifier is

$$\frac{Q_o}{P_i} \simeq - \frac{1}{R_1} \frac{1 + R_2 Cs}{1 + \frac{Ts}{2e^{-Ts}}} \qquad (3\text{-}4)$$

Our concern is the right hand terms in the numerators of eqns. (3-3) and (3-4). The lead term in the pressure relation can be eliminated by setting $R = R_2$ i. e. $R_3 = 0$.

This however would force the time constant in the flow relation to become very large, since from equation (3-2)

$$R_2C \simeq g\frac{T}{2}\frac{1}{(\frac{2}{R_1} + Y_i)Z_o} \qquad (3\text{-}5)$$

(where it has been presumed that $\frac{2R_2}{R_1} >> 1$) and Z_o is not too large. This is nevertheless the most typical design.

The response of pressure with this design is good as seen in eq. (3-3) and the flow response is of no consequence if linearity holds. The physical volume which gives the C is very large but usually this is tolerable. For other than the tiniest input amplitudes or the slowest of input rates of change however, the fluidic amplifier saturates and these results do not apply. The compliance volume has to be changed to its new steady-state pressure before equilibrium is achieved. Eq. (3-4) would have this occur fairly quickly because of an enormous flow Q_o. In fact, however, the flow Q_o saturates usually at a small fraction of the linear-model value and the volume is changed and equilibrium achieved at a much slower rate. The response is said to be severely rate-limited or amplitude dependent.

The critical time constant R_2C can be reduced, shortening the charging process by introducing a non-zero R_3.

The lead term in $\frac{P_o}{P_i}$ hurts, but in the limit $R_3 = R(R_2=0)$ the lead term vanishes again.

$$\frac{P_o}{P_i} \simeq -\frac{R}{R_1}\,\frac{1}{1+\frac{Ts}{2e^{-Ts}}} \qquad (3\text{-}6)$$

$$\frac{Q_o}{P_i} \simeq \frac{1}{R_1}\,\frac{1}{1+\frac{Ts}{2e^{-Ts}}} \qquad (3\text{-}7)$$

The associated compliance is

$$C = \frac{gT}{2(R + Z_o)}$$

which could be either smaller or larger than with the conventional design depending on the ratio Z_o/R. The steady-state input and output impedances is the same with all designs.

This design clearly is superior to the conventional one largely because the saturation problem is virtually eliminated. In simple terms the improvement results from the need to charge the compliance to only a tiny fraction of the pressure needed for the conventional design. With this spur toward strikingly improved design, a nearly optimum design is presented in the next section.

3.2 Basic Optimal Design of the Operational Amplifier

The nominal representation of the five-stage amplifier is a constant gain g with time delay T, and real constant input and output admittances Y_i and $1/Z_o$ respectively. It is well known in control theory that feedback placed around a pure delay cannot hasten the response. The optimal design gives a closed-loop response which is itself a pure delay of the same time T but a different overall gain as desired. This then is a goal of the actual closed-loop design. Were this the only goal, however, there would be no point in using feedback at all since it could be achieved simpler with a pressure divider cascaded into the five-stage amplifier. We wish however to vastly increase the output admittance, that is to render the circuit insensitive to wide variations in load. Decreasing the input admittance also is desirable. Finally we wish to increase the linearity of the circuit.

For the moment let us forget considerations of flow (partly by blocking the load) and attempt to achieve the desired gain characteristics using feedback path compensation and alternatively forward path compensation. Referring to figure 5 it can be seen that the necessary feedback compensator is

$$H(s) = \left(\frac{1}{K} - \frac{1}{g}\right) e^{Ts}$$

which is impossible since it requires an anticipator, a time advance. The necessary forward path compensator, however is achievable.

$$G(s) = \frac{K}{g} \frac{1}{1-kKe^{-Ts}} = \frac{K}{g} [1+kKe^{-Ts}+(kK)^2e^{-2Ts}+(kK)^3 e^{-3Ts}+....]$$

$$kK = 1 - \frac{K}{G(o)g}$$

The choice G(o) = 1 is not practical since g >> K the value of kK is virtually one, and the step response of G(s) is the staircase function shown in figure 5(d).

This staircase function suggests a travelling wave device, in particular a resonating blocked-ended tube. The impedance (ratio of pressure to flow) with a round-trip wave delay of T seconds is (from standard methods) as seen at the driving end.

$$Z = Z_c \text{ Coth } \frac{Ts}{2} = Z_c \frac{1 + e^{-Ts}}{1 - e^{-Ts}}$$

where Z_c is the characteristic impedance of the cross-section.

Now we add a flow resistor in series at the driving end with resistance equal to Z_c, the net impedance then becomes

$$Z = Z_c + Z_c \frac{1 + e^{-Ts}}{1 - e^{-Ts}} = \frac{2Z_c}{1 - e^{-Ts}} \qquad (3\text{-}8)$$

which is of the same form as G(s) (with kK = 1).

This tube is incorporated into the circuit of the operational amplifier as shown in figure 6, as the only nominally dynamic element. The circuit is not ideal, however, because the various impedances and the gain g are finite. The transfer function from input to output pressures can be shown to be

$$\frac{e_o}{e_i} = -\frac{R_4}{R_1}\frac{1}{\Delta}\left[\left(ge^{-Ts} - \frac{Z_o}{R_4}\right)\left(1 + R_2(Y + Y_i)\right)\right]$$

$$\Delta = \left[g - \frac{Y_c R_b}{2}\right]e^{-Ts} + \left(Y_i + \frac{Y_c}{2}\right)R_b + r$$

$$R_b = \left[Z_o + (R_2 + R_4)(1 + Z_o Y_o)\right] + \left(\frac{R_2}{R_1'} + \frac{R_2}{R_1}\right)\left[R_4(1 + Z_o Y_o) + Z_o\right]$$

$$r = \left(1 + \frac{R_4}{R_1'} + \frac{R_4}{R_1}\right)(1 + Z_o Y_o) + \frac{Z_o}{R_1} + \frac{Z_o}{R_1'}$$

The requirement kK = 1 corresponds to settling the delay term in Δ equal to zero, that is

$$R_b Y_c = \frac{R_b}{Z_c} = 2g$$

For our particular design we choose

$$R_1' = R_1 = 0.1R_4$$

giving

$$R_b = (1 + \frac{2R_2}{R_1})Z_o + (2R_2 + 10R_1)(1 + Z_oY_o)$$

$$r = 21(1 + Z_oY_o) + \frac{2Z_o}{R_1}$$

$$\frac{e_o}{e_i} = -10\frac{e^{-Ts} - \frac{Z_o}{10R_1}\left[\frac{1 + R_2Y_i}{g} + \frac{R_2}{R_b}(1 - e^{-Ts})\right]}{1 + \frac{2Y_i}{Y_c} + \frac{r}{g}}$$

The left hand terms in the numerator and the denominator represent the non-ideal effects of finite gain and impedances. The right hand term in the numerator represents the direct transfer of the input to the output through the nominal feedback paths. Since g is very large and the magnitude of the putput impedance Z_o does not exceed R_1 the first term in the brackets can be seen to be trivial.

To make the middle term in the denominator no greater than a one percent effect, we require

$$|Y_i| < \frac{Y_c}{200}$$

The same restriction on the right hand term is

$$r < \frac{g}{100}$$

From the data the magnitude of Y_i is about 0.4 in^5/lb.sec. giving $Y_c > 80$ in^5/lb.sec. A much larger value of Y_c cannot be tolerated however since it would require an excessively large cross-sectional area. The value

$$Y_c = \frac{\text{Area}}{\rho C} = 86.2 \text{ in}^5/\text{lb.sec.}$$

was chosen corresponding to a diameter of 0.406 inch. Another physical difficulty is making resistors with small resistances. Since R_b is essentially fixed at this point, making the smaller of R_1 and R_2 as large as possible is satisfied by giving them the same value or $R_1 = R_2$.

The load admittance Y_o has been selected as zero since this is the easiest condition to achieve. With all these conditions assuming g = 2500, we have

$$R_b = \frac{2g}{Y_c} = 58.0 \frac{\text{lb.sec.}}{\text{in}^5} = 3Z_o + 31R_1 \simeq 5.1 + 31R_1$$

Therefore $R_1 = 1.738 \frac{\text{lb.sec.}}{\text{in}^5}$; $r = 24.4$

The resistance can be achieved with adequate linearity.

Considering Z_o and Y_i as real numbers (they actually are complex numbers, frequency dependent) the overall gain becomes

$$\frac{e_o}{e_i} = -10\,\frac{e^{-Ts} - 0.0029(1 - e^{-Ts})}{1 + 0.0094 + 0.0049}$$

Which is quite close to the ideal of $-10e^{-Ts}$. The input admittance is

$$\frac{Q_i}{e_i} = \frac{1}{R_1\Delta}\,[1 + ge^{-Ts} + (Y + Y_i)(Z_o + R_2 + R_4)]$$

$$\frac{Q_i}{e_i} \simeq \frac{1}{R_1}\,[e^{-Ts} + \frac{Z_o + R_2 + R_4}{R_b}\,(1 - e^{-Ts})]$$

$$\frac{Q_i}{e_i} \simeq \frac{1}{R_1}\,[0.65e^{-Ts} + 0.35] = 9.376e^{-Ts} + 0.202\ \frac{in^5}{lb.sec.}$$

The output admittance is

$$\frac{Q_o}{e_o} = \frac{\Delta/Z_o}{(Y+Y_i)[R_2+R_4+(\frac{R_2}{R_1} + \frac{R_2}{R_1})R_4] + 1 + \frac{R_4}{R_1}}$$

$$\frac{Q_o}{e_o} = \frac{1}{Z_o[0.908(1-e^{-Ts}) + 0.0065]}$$

The principle virtue of an operational amplifier is its large output admittance relative to the input admittance. The ratio actually is very large, however, only for low frequencies (and certain high frequencies). For zero frequency

$$\left(\frac{Q_o}{e_o}\right)_{\omega=0} = \frac{1}{0.0065Z_o} = 90\ \frac{in^5}{lb.sec.}$$

It is useful conceptually now and practically later on to view the operational amplifier in the feedback loop form. This is possible if the very small second term in the numerator of the gain characteristic is neglected (corresponding to neglect of the signal propagated from input to output via the feedback resistor channel). The open loop gain is for $R_1' = R_1$,

$$\ell = \frac{-ge^{-Ts}}{(Y+Y_i)R_b+r} \simeq \frac{-ge^{-Ts}}{YR_b} = \frac{-ge^{-Ts}}{g(1-e^{-Ts})}$$

when Y is the admittance of the shunt controller (reciprocal of the Z of eq. (3-8) when the nominal parameters are assumed). The forward path gain is

$$f = \frac{R_t}{R_1}\,\ell$$

The closed loop then becomes

$$\frac{e_o}{e_i} = \frac{R_t}{R_1}\,\frac{\ell}{1-\ell} \simeq -\frac{R_4}{R_1}\,\frac{ge^{-Ts}}{YR_b+ge^{-Ts}} = -\frac{R_4}{R_1}\,e^{-Ts}$$

where the substitution $Y_cR_b = 2g$ has been made. This agrees with the earlier result.

To simplify further investigation consider the open loop gain to be the ratio of two terms. The numerator is the forward path transmittance of the five-stage amplifier, which for the nominal model has a Nyquist frequency response

as shown in figure 25. The denominator predominantly represents characteristics of the feedback path and compensation (plus a relatively small influence of the input and output admittances of the five-stage amplifier. For its nominal model the Nyquist plot is also a circle of radius g but centered at +1 (see figure 28). The ratio of the two circles is a straight line with real part of $-\frac{1}{2}$. This is of course the M-circle which gives a closed loop frequency response of magnitude ratio unity at all frequencies.

The actual transmittance of the five-stage amplifier (not known very precisely) is plotted in figure 25. The denominator of the actual open loop gain also differs from its ideal model, largely because of inertance in all of the nominally resistive elements, but because of the compliances between the control ports and the resonance tubes.

The inertance of resistors R_1, R_1', R_2 and R_4 have inertances proportional to their resistances. That is, all have impedances of the form

$$Z = \frac{R}{\tau s + 1}$$

With the same time constant $\tau = 1.0 \times 10^{-4}$ secs. This gives a break frequency of 1590 Hz. The consequent Nyquist plot of R_b which depends somewhat on the dynamic values of Z_o is

given in figure 29.

The admittances Y should be modelled more closely than in the nominal model by

$$Y = Cs + \frac{Y_c}{1 + \tau_p s + \tanh \frac{Ts}{2}}$$

where τ_p is the inertive time constant of the porous disks. According to Anderson†. The break frequency of sintered porous media (which presumably depends largely on the void fraction) should be about 4000 Hz, giving $\tau p = 0.4 \times 10^{-4}$ secs. The compliance C is

$$C = \frac{\text{volume}}{\text{abs. pressure}} = \frac{0.0141}{14.7} = 9.59 \times 10^{-4} \frac{in^5}{lb}$$

The term Y is plotted in figure 30, and the product YR_b in figure 31.

The corrected Nyquist plot of the loop gain is given in figure 32, is seen to differ from the straight line ideal in a minor way below about 1000 Hz and probably to vary substantially above 1000 Hz (since the actual characteristics of the five-stage amplifier were not measured above 1000 Hz). The assumption of the ideal model has been made with g = 2500, $T = 3.06 \times 10^{-4}$ sec., $Y_i = 0.4$ $in^5/lb.sec.$, $Z_o = 1.45$ $lb.sec^2/in^5$.

†Anderson, John E., "Acoustical Impedance Characteristics of Sintered Stainless Steel", Journal of Acoustical Society of America, Vol. 36, No. 5, May 1964.

The measured phase angle of the five-stage amplifier increases more slowly for low frequencies than for moderate frequencies. Further the prospects for good response at quite high frequencies are poor. These facts combine to suggest a modified compensator which is more nearly optimum as described in Chapter 5.

4. EXPERIMENTAL STUDY

4.1 Design Details of the Operational Amplifier

The resistance values $R_1 = R_1' = R_2 = 1.738$ lb.sec./in^5 and $R_4 = 17.38$ lb.sec./in^5 are large enough to permit practical construction using etched metal laminates, compatible with the basic construction of the AM-12 amplifier. The shunt resistance $R_3 = 0.0116$ lb.sec./in^5 is much too small and resort was made to sintered porous plates.

The etched metal laminates chosen are all 0.003 inch Berylium copper shown full size in Figure 11. The resistors R_4 are single channels 0.003 inch deep, 0.0528 inch wide and 0.80 inch long. The resistors R_1, R_1' and R_2 are comprised of three parallel channels each 0.003 inch deep, 0.066 inch wide and effectively 0.300 inch long. The channels for R_1 and R_1' are actually bent, but their length was corrected by plotting flow and equi-pressure lines. The resistance values can be checked by using the formula

$$R = \frac{12\mu\ell}{nwt^3}$$

in which t is the depth, ℓ the length, w the width and n the number of parallel channels. This formula was derived simply from the assumption of parabolic profiles and negligible edge effects (w >> t). The flow becomes fully developed in an exceedingly short distance for pressure drops

in the range of interest.

The inertance of the resistances can be derived as

$$I = \frac{3\rho\ell}{nwt}$$

where the factor 3 results from the parabolic profile (the factor would be unity for a slug profile and the kinetic energy equals $\frac{1}{2} IQ^2$). The time constant for the resistance thus is

$$\tau = \frac{I}{R} = \frac{t^2}{4\nu} = 1.00 \times 10^{-4} \text{ sec.}$$

and the associated break frequency is

$$f_b = \frac{1}{2\pi\tau} = 1590 \text{ Hz}$$

at which the pressure drop leads the flow by 45°. The frequency interestingly is independent of w, ℓ and n and applies to R_4 as well as R_1, R_1' and R_2.

The porous plates were supplied by Alcan Metal Powders, Inc. They are $\frac{1}{8}$" thick and formed from bronze particles. The resistance to flow per square inch was supposed to equal the surge impedance of air, ρC, as desired, but measurements using a special rig revealed that the resistance was slightly higher. To compensate, the area of the plate exposed to flow was made a little larger than the area of the resonant cylinder.

The equation $\frac{\rho C}{A} = R_3 = 0.0116$ lb.sec./in^5 gives a cylinder area A of 0.406 in^2. The length of the cylinder, chosen (in the basic design) to give a one wave delay time T/2 is 2.02 inches. The inertive break frequency for the porous plates is approximated at 4000 Hz as stated in section 3.2.

The original design of the entrance to the control port is shown in figure 12(a). The operational amplifier proceeded to screech violently at one or more high frequencies. The solution is shown in figure 12(b). The explanation is that even a tiny coupling between the dynamic head of the exceedingly weak fluid jets emanating from the passages of the resistance R_2 and the control port pressure can give a loop gain exceeding unity at high frequencies and phase lags. The coupling is virtually eliminated by the redesign.

4.2 Static Gain Characteristic Test

The schematic for the static gain characteristic test is shown in figure 8. The power jet entering the supply port (not shown) was maintained at 10 psi. In order to maintain a virtually zero pressure at the control ports, the input to the resistances R_1 were kept at an average pressure of -0.3 psig. The other two inputs leading to resistances R_1' were open to atmosphere. The differential output pressure was measured for various input differential

pressures. The plot is shown in figure 34. This is of course a "push-pull" operation.

The results show a pressure gain of 7.7 in the linear range which is lower than the value for which it was designed. The reason for this could be largely due to the buckling of the etched Berylium copper plates which would bring about two effects. The first would be to allow flow from one channel to another. To avoid this, vacuum grease was used which caused blocking of the resistances. The other and more important is that the values of the resistances are inversely proportional to the third power of the thickness (see section 4.1) and a slight buckling effect could drastically change their value. In addition the width of the resistances would also tend to increase with buckling. The values of these resistances could not be ascertained, therefore, as the buckling would depend on the manner the plates were clamped.

4.3 Frequency Response of the Operational Amplifier

The schematic for the frequency response test is shown in figure 9. Semi-conductor strain gage pressure transducers were used because of their high sensitivity and small size. A Tetronix Q-plug-in unit was used to observe the input and output signals and a Wave-Analyzer (not shown) for measurements of magnitudes of the pressures. Here too, as in the

static gain test, the input pressures were maintained at an average of -0.3 psig and the supply pressure at 10 psi. The pressure transducer (or dummy transducers) served to block the output ports.

Pressures at the input and output ports were measured at various frequencies and their magnitude ratio plotted on a linear scale as shown in figure 35. The response suffers a dip at about 300 Hz which would be expected at low frequencies since the basic design assumes a linear increase in phase which is not so. The phase lag of the cascade amplifier increases slowly at low frequencies and more rapidly at higher frequencies. The dip is followed by a resonance at about 700 Hz compared to the predicted value at about 900 Hz (see figure 33). The gain up to 1200 Hz is about 4.2 which is fairly lower than the designed value of 10. This disagreement as discussed in section 4.2 is largely due to the resistances not being of the calculated value. The second and third resonance occur at about 1500 Hz and 2950 Hz which would be for a phase lag of 540° and 900° respectively.

5. MODIFIED OPTIMAL DESIGN OF THE OPERATIONAL AMPLIFIER

5.1 The Modified Model

The measured pressure gain of the cascade amplifier, figures 25 and 26 shows approximately a constant magnitude but the phase lag does not increase linearly with frequency as it does in the basic model. Rather the phase lag increases slowly at low frequencies and more rapidly at higher frequencies. In consequence the closed-loop frequency response of the operational amplifier design assuming a linear increase in phase, suffers a dip followed by a resonance (since a mean delay time T was chosen).

The measured gain characteristic can be represented (to within the unfortunately large experimental error) by

$$G_f(s) = g \frac{s^2 - 2\zeta\omega_n s + \omega_n^2}{s^2 + 2\zeta\omega_n s + \omega_n^2}$$

This transfer function, with two complex zeroes in the right-half plane placed symmetrically opposite two complex poles in the left-half plane, produces a circle for its Nyquist plot just as does the nominal e^{-Ts}. Its main disadvantage is that as $\omega \to \infty$ there is only one revolution of the circle. The data can be well matched since it extends to less than 180° lag but we know from prior considerations, closed-loop experimental results and informal

independent reports that the phase lag makes considerably more than one revolution before the amplitude becomes significantly attenuated. Its assumption as the basis for optimal design should work well up to 1000 Hz or possibly 2000 Hz, but opens the real possibility of higher frequency instabilities. Such instabilities should be damped without significantly impairing low frequency behaviour, however by introducing quite small volumes at the summing functions. Since the interest is in demonstrating the potential of optimal design techniques, the use of the modified model seems appropriate.

The series compensator (see figure 7(a)) which gives the least integral square error in response to slip areas is merely a constant for any system with unity gain, regardless of how the phase lag increases with frequency. When placed in the unity feedback form of figure 7(b) the optimal forward path compensator becomes

$$G_c(s) = \frac{s^2 + 2\zeta\omega_n s + \omega_n^2}{g + \zeta\omega_n s}$$

Note the cancellation of the right-half-plane but not the left-half-plane singularities of $G_f(s)$, common to optimal controllers. The closed-loop response can be seen to be directly proportional to $G_f(s)$ as desired.

The desired compensation $G_c(s)$ can be achieved by

using a shunt admittance similar to and substituting for the resonance tube of the basic design of section 3.2. An inertance is added to the resistance and the resonator tube is charged to a simple compliance as shown in figure 7(c). The admittance of this combination is

$$Y = \frac{Cs}{1 + RCs + ICs^2}$$

The resonant frequency $1/\sqrt{IC}$ is set at ω_n which is the π/T of the basic design. At the resonant frequency it is desired to have the admittance to be the same as in the basic design which was labelled Z_c, so that

$$R = Z_c$$

$$C = \frac{2\zeta}{Z_c \omega_n}$$

$$I = \frac{Z_c}{2\zeta\omega_n}$$

For $\zeta = \pi/4$ the compliance C requires precisely the same volume as did the resonant tube although of course a shorter and fatter geometry would more nearly approach the lumped-element ideal.

The values which best fit the data as shown in figure 26 is about $f_n = \omega_n/2\pi = 1130$ Hz and $\zeta = 0.33$, fortunately requiring a smaller volume of 0.118 in^3. Since $Z_c = 0.0116$ lb.sec./in^5 as before one obtains $C = 0.00802$ in^5/lb. and

$Z = 2.48 \times 10^{-6}$ lb.sec^2/in^5. Since the inertance of the porous disk is about 0.46×10^{-6} lb.sec^2/in^5, an added inertance of about 2.02×10^{-6} lb.sec^2/in^5 is needed.

5.2 Design Details of the Modified Model

The modified design requires an added inertance of 2.02×10^{-6} lb.sec^2/in^5. This can be achieved with one or two parallel modest size holes in a disk inserted between the control port and the porous plate with sufficient space on either side for distribution of the flow. This was not actually carried out with the proper design (it worked predictably with an improper design which followed an analytical slip). If it is done with one hole in a very thin disk (say < 0.016 inch) the inertance is about $4 \times 0.613\rho/\pi d$ giving the diameter $d \tilde{=} .044$ inch. The diameter should increase if the disk is thicker.

The desired volume of 0.118 in^3 results from a length of 0.91 inch; since the length is of the same order as the diameter of the basic cylinder the cylinder area need not be changed.

6. SUMMARY

The purpose of this study was to design a nearly optimum operational amplifier using a commercially available cascaded proportional amplifier. It was shown that to achieve an optimal design it was only possible to have forward path compensation, unlike the conventional design of operational amplifiers.

The transfer function of the loop gain of the gain block was represented nominally as a constant gain and time delay for the Basic Optimal Design. The actual transmittance however shows that the phase lag does not increase linearly with frequency. It increases slowly for low frequencies and then rapidly for moderate frequencies which would cause a drop in the gain at a certain low frequency and then a resonance. This predicted behaviour was seen in the experimental results. Moreover the prospects of a good response of this design are poor at high frequencies. These together suggested a modified compensator. The gain characteristics of the proportional amplifier were therefore represented by a second transfer function which also has a circle for its Nyquist plot just as the nominal representation of time-delay.

The compensator of the Modified Model uses a shunt admittance (similar to the resonance tube of the Basic Design)

with an added inertance. The experimental testing of the modified model was not carried out with the proper design. However, it worked predictably with an improper design (which was due to an analytical slip) which gave an indication that this design could well achieve a very near-optimization of the operational amplifier.

Both static and dynamic data are marred by feedback and input resistances different from the design values. The deviations were not directly measurable and apparently resulted either from undesired leakages or blockages (the latter by the vacuum grease) or warpages. Their severity, obvious from the unbalance and error in the static gain measurements, renders the dynamic experiments of qualitative significance only. It is hoped that corrections will be made in the future to demonstrate the usefulness of the concepts presented herein.

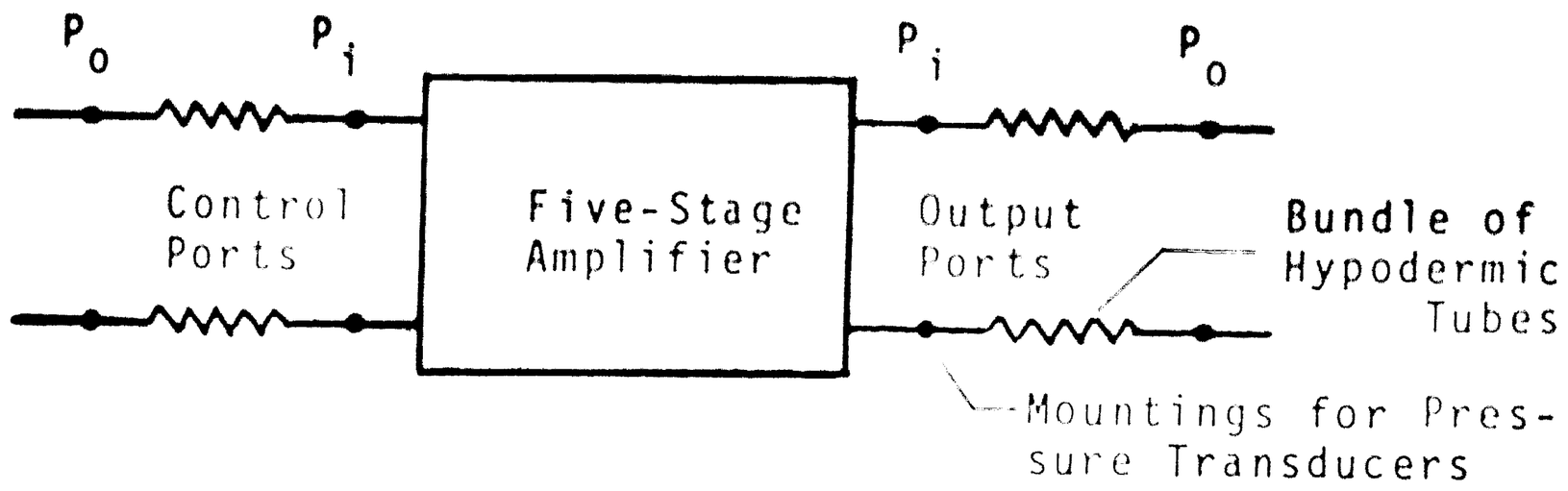

Figure 1(a) Measurement Scheme

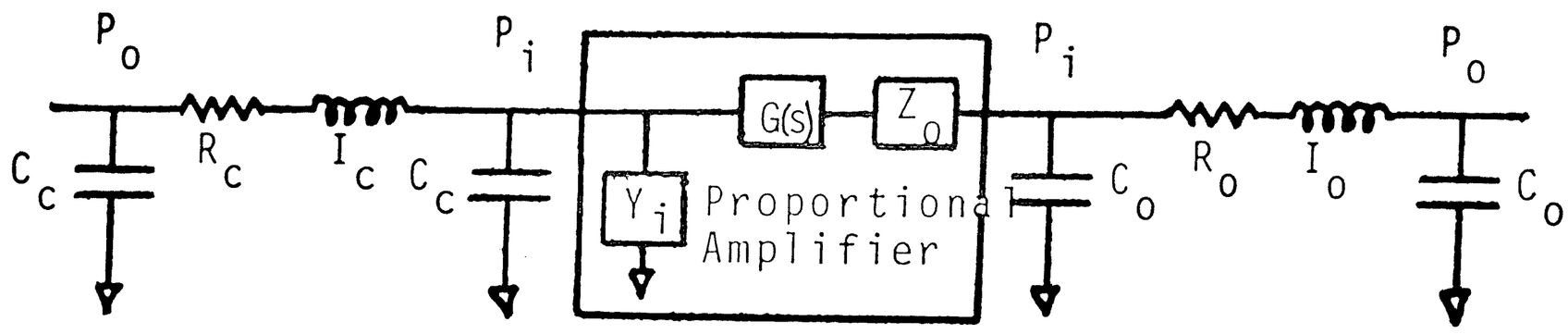

Figure 1(b) More Accurate Model of Circuitry

Figure 1. Electrical Analogy of the Circuitry Used in Determining the Characteristics of the Five-Stage Amplifier.

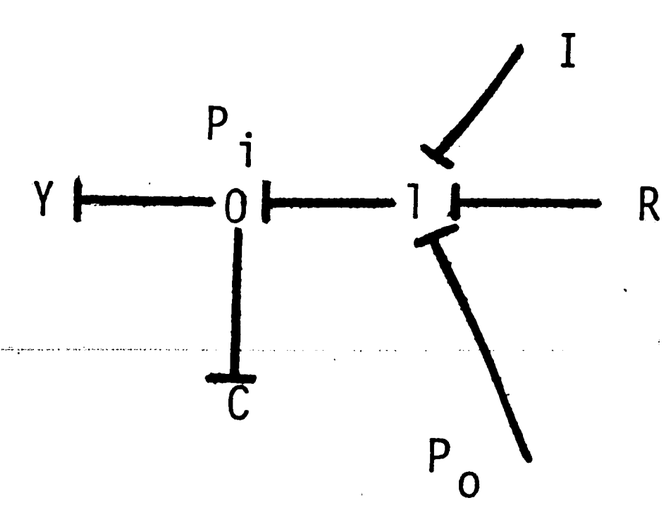

Figure 2. Bond Graph of Circuitry Shown in figure 1(b).

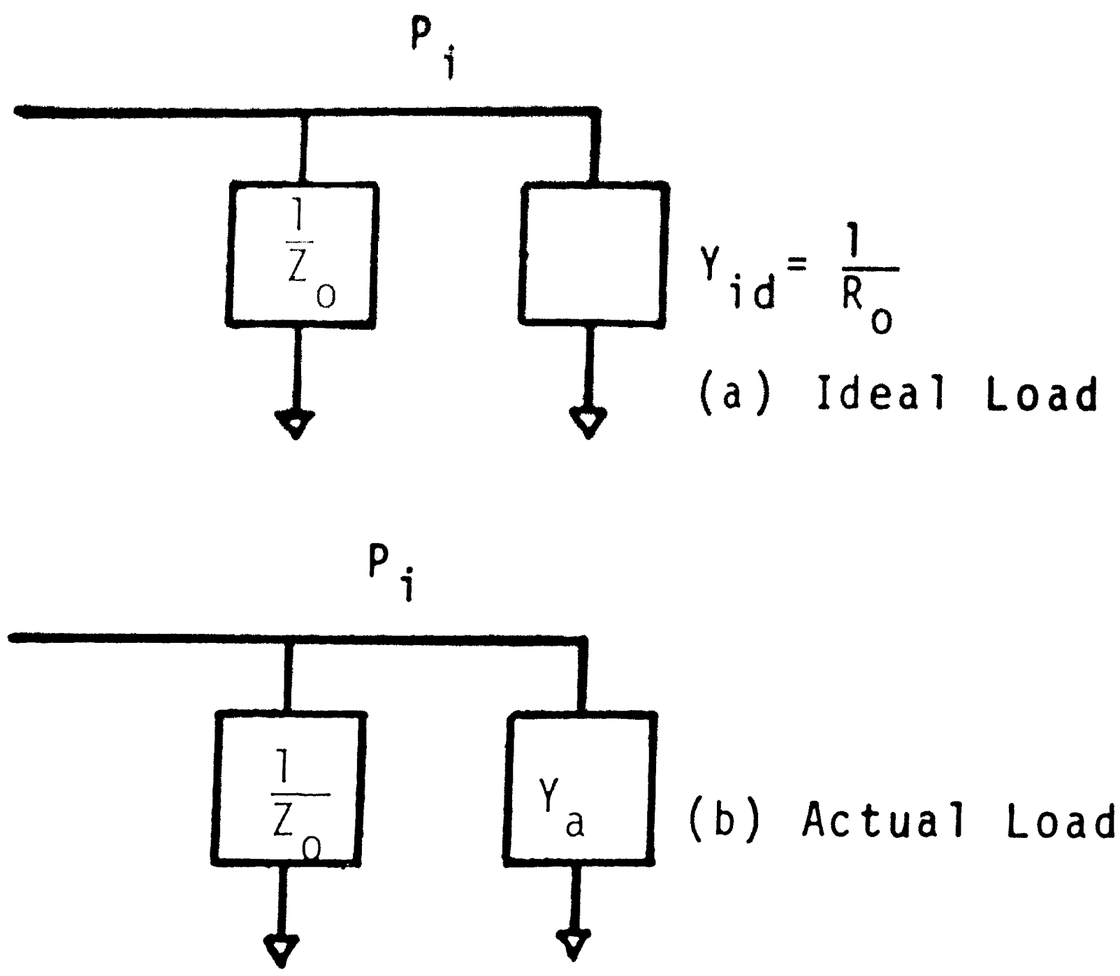

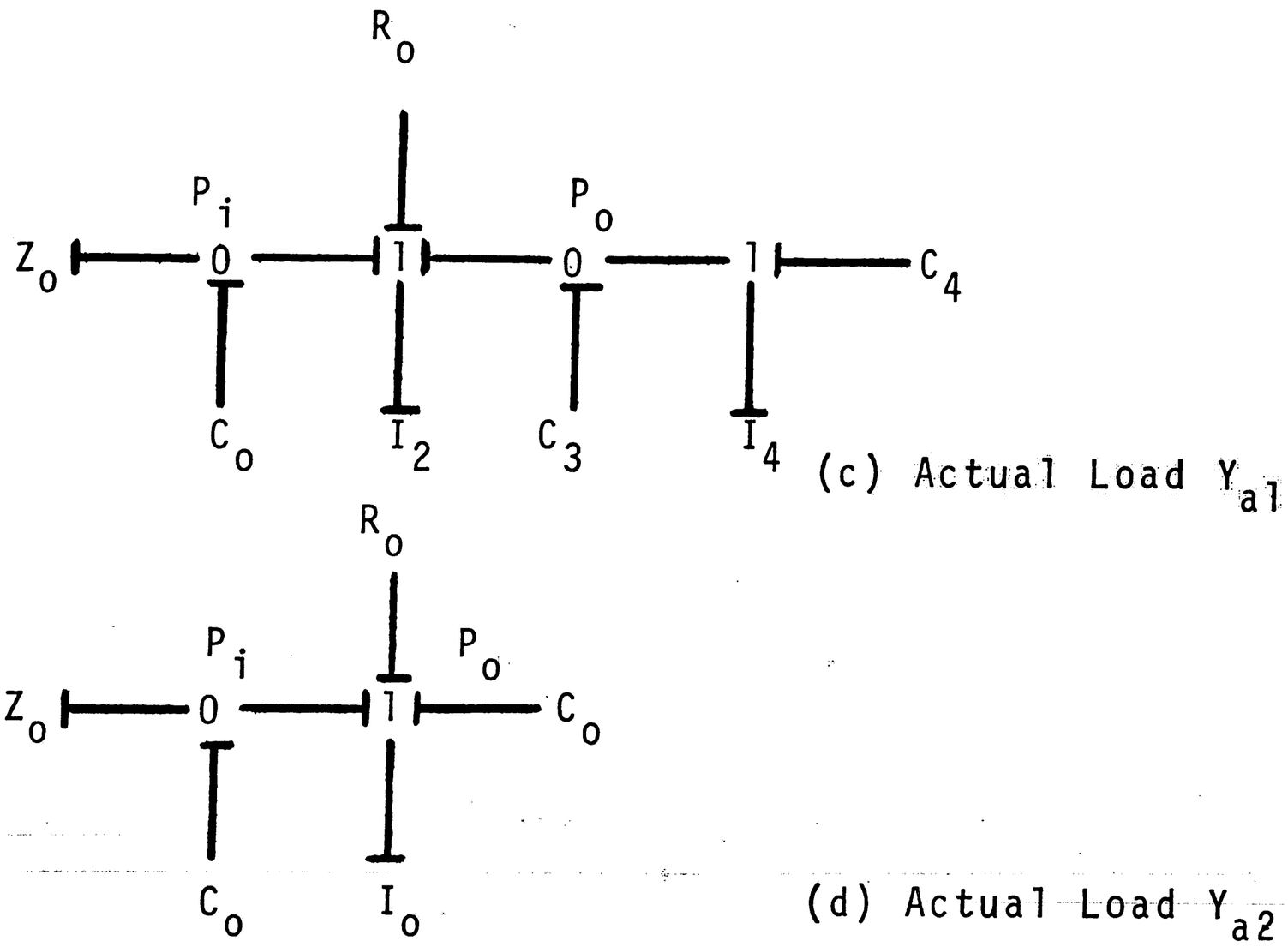

Figure 3. Loads Used for Determining the Characteristics of the Five-Stage Amplifier.

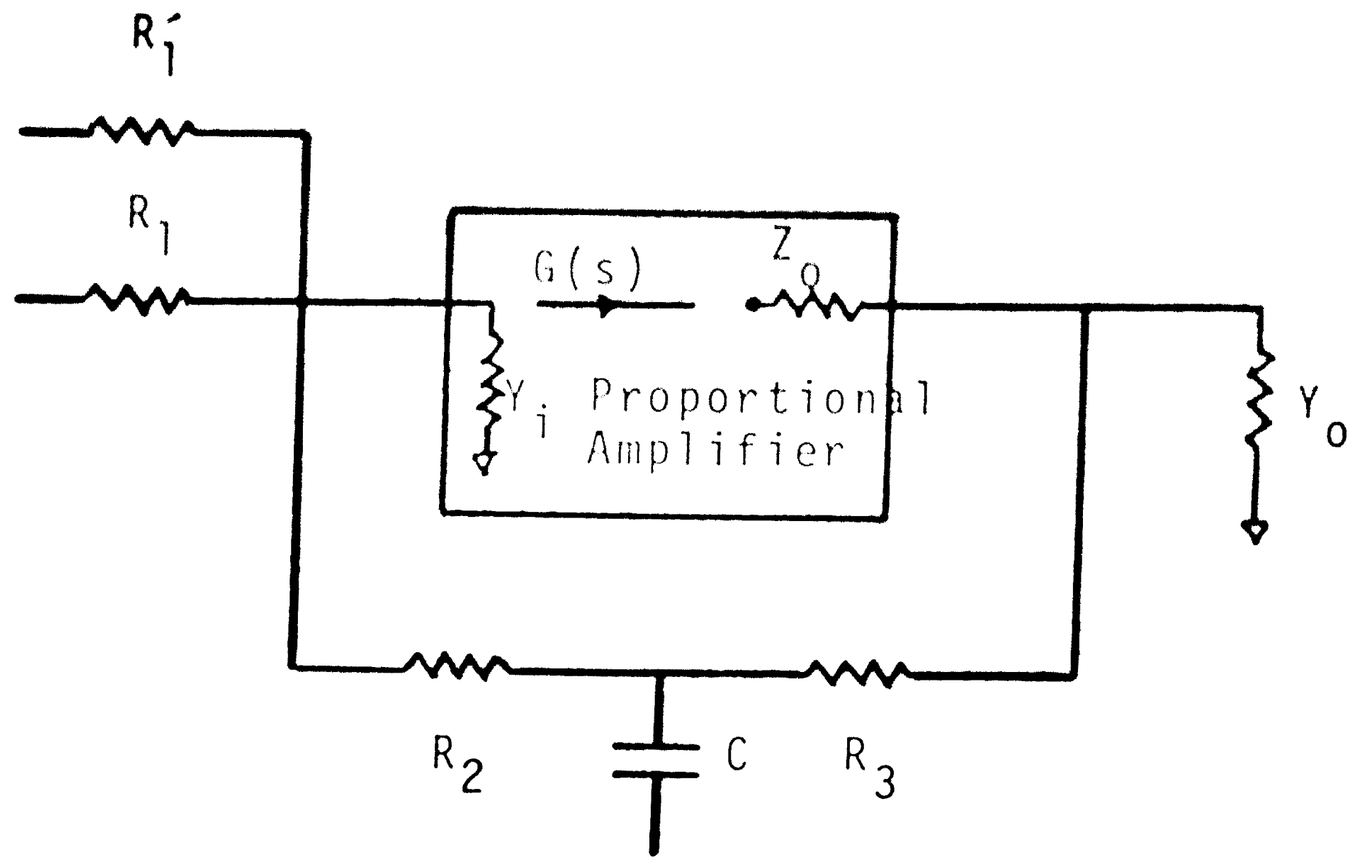

(a) The Conventional Operational Amplifier

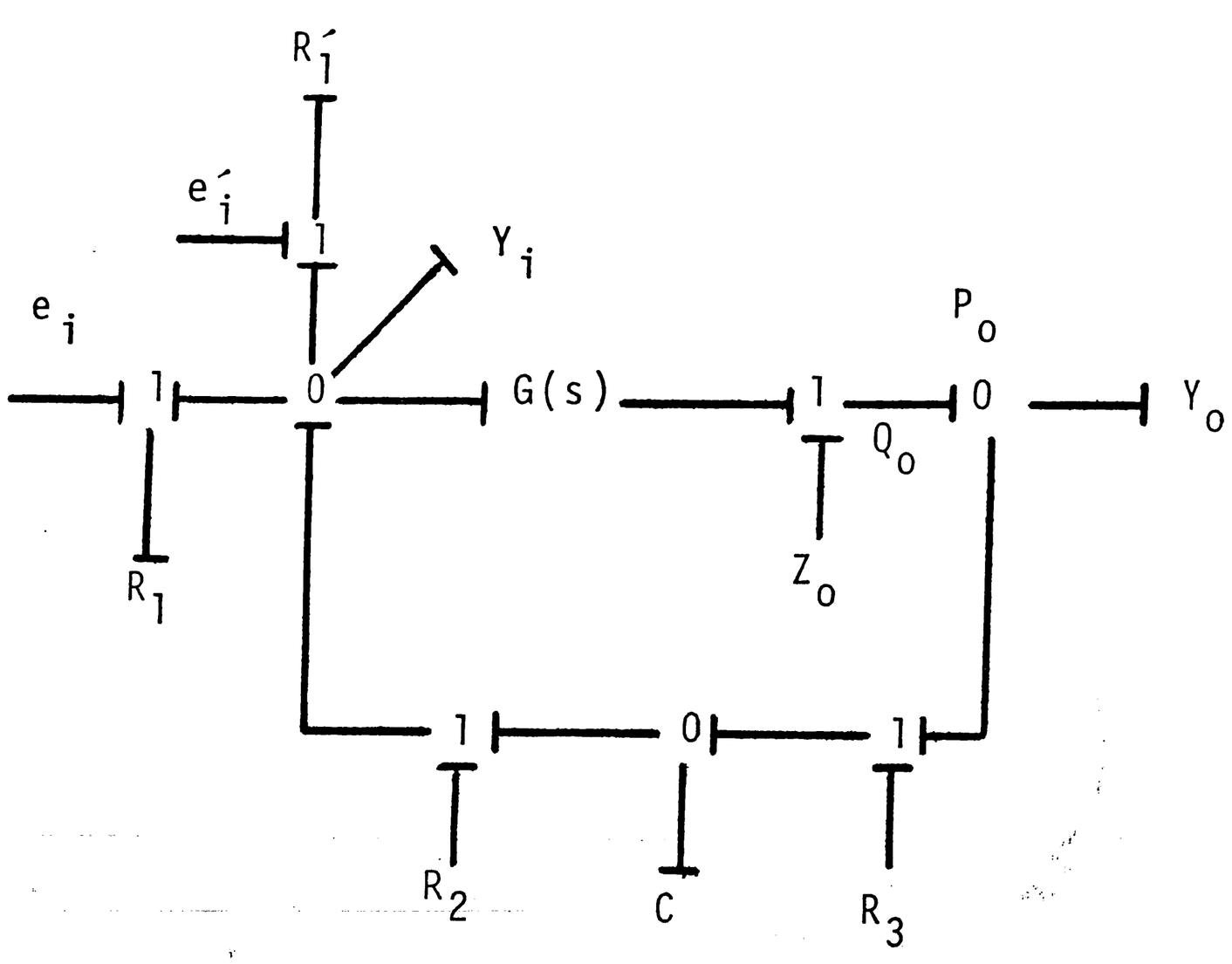

(b) Associated Bond-Graph of the Conventional Operational Amplifier

Figure 4. The Conventional Operational Amplifier.

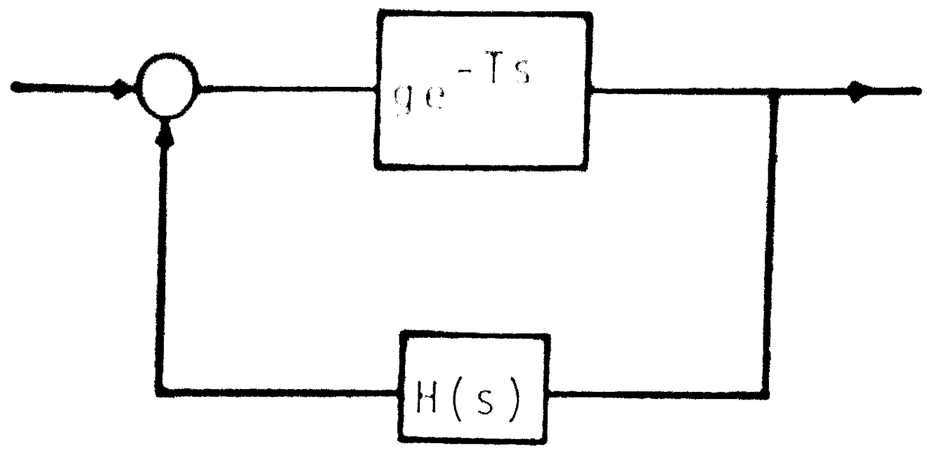

(a) Feedback Compensation

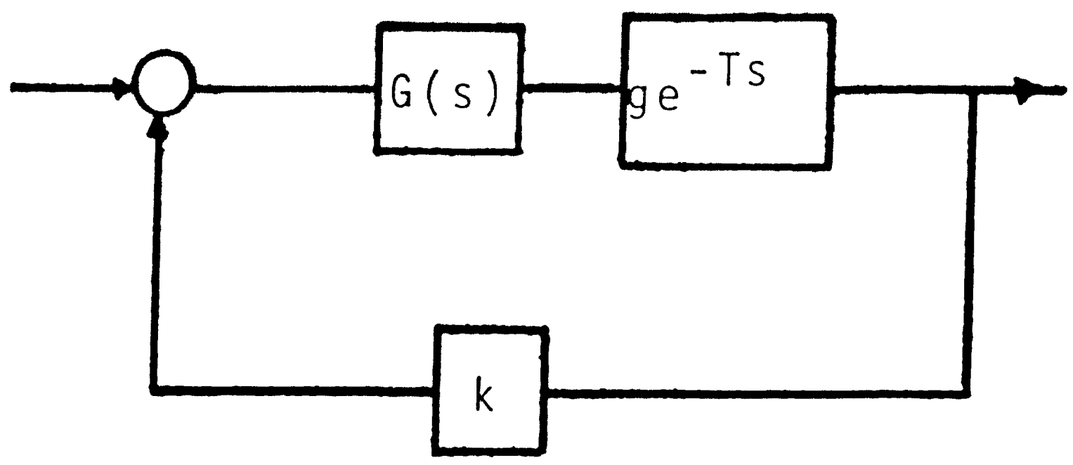

(b) Feedforward Compensation

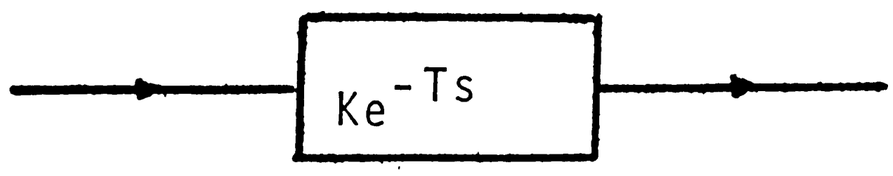

(c) Desired Closed-Loop Behavior

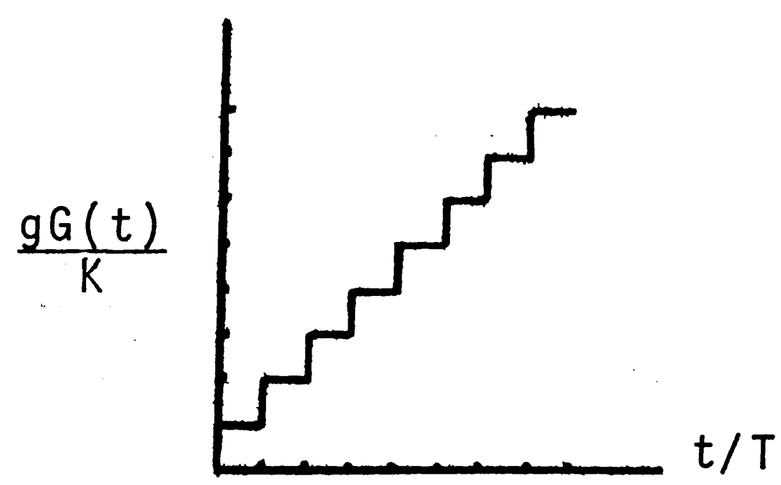

(d) Slip Response of Resulting G(s)

Figure 5. Concepts of Feedback Path and Forward Path Dynamic Compensation.

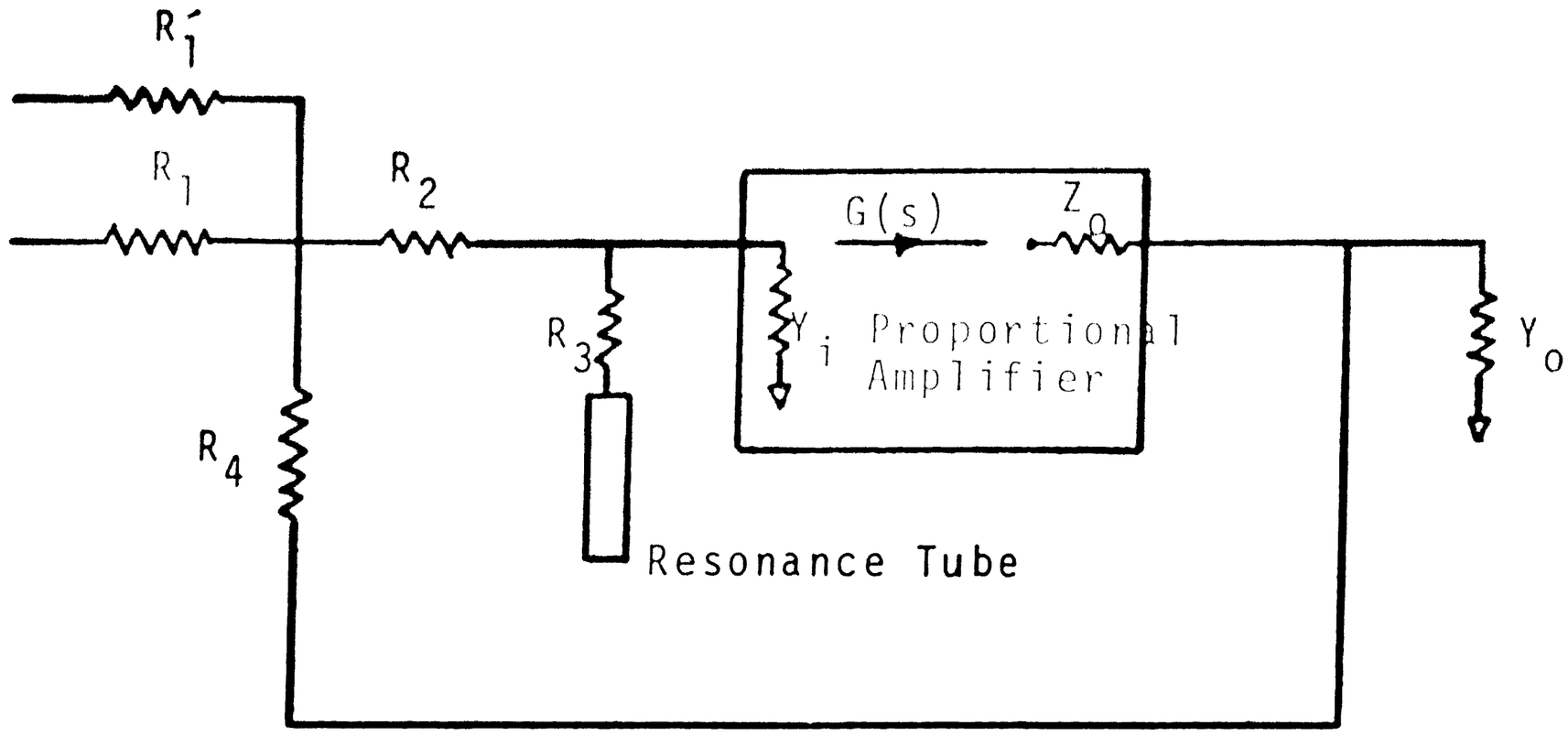

(a) Circuitry of the Basic-Optimal Operational Amplifier

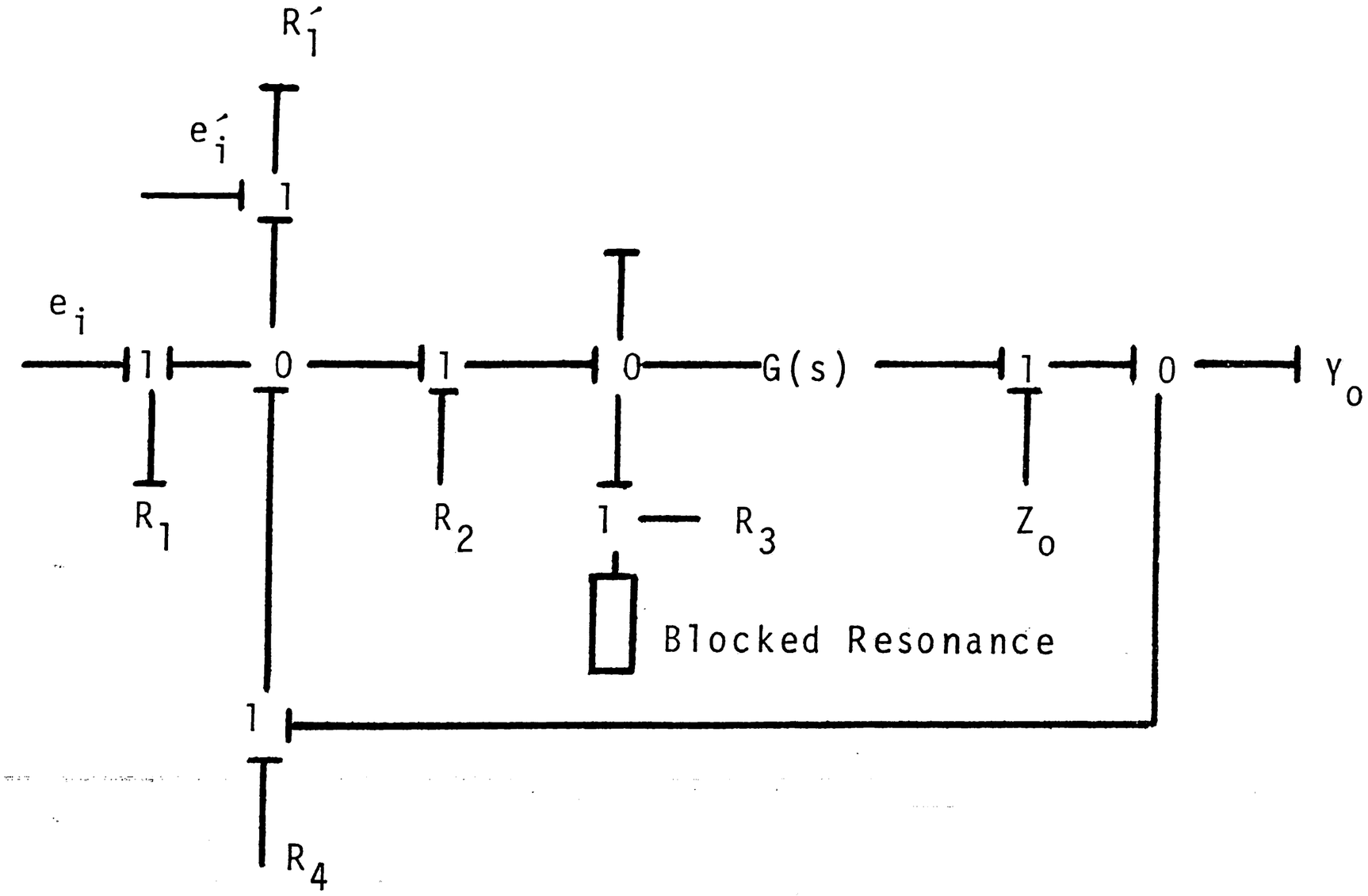

(b) Associated Bond-Graph of the Operational Amplifier

Figure 6. The Basic-Optimal Operational Amplifier.

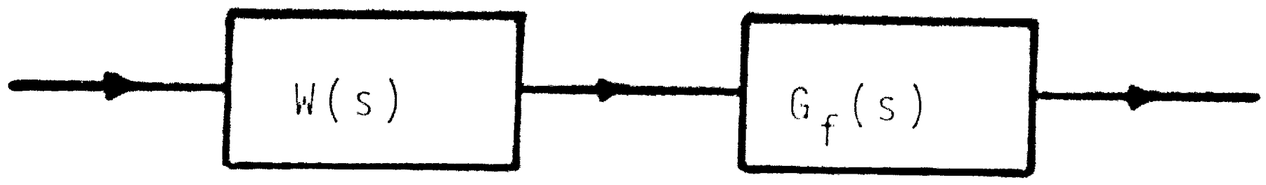

(a) Concept of Series Compensator

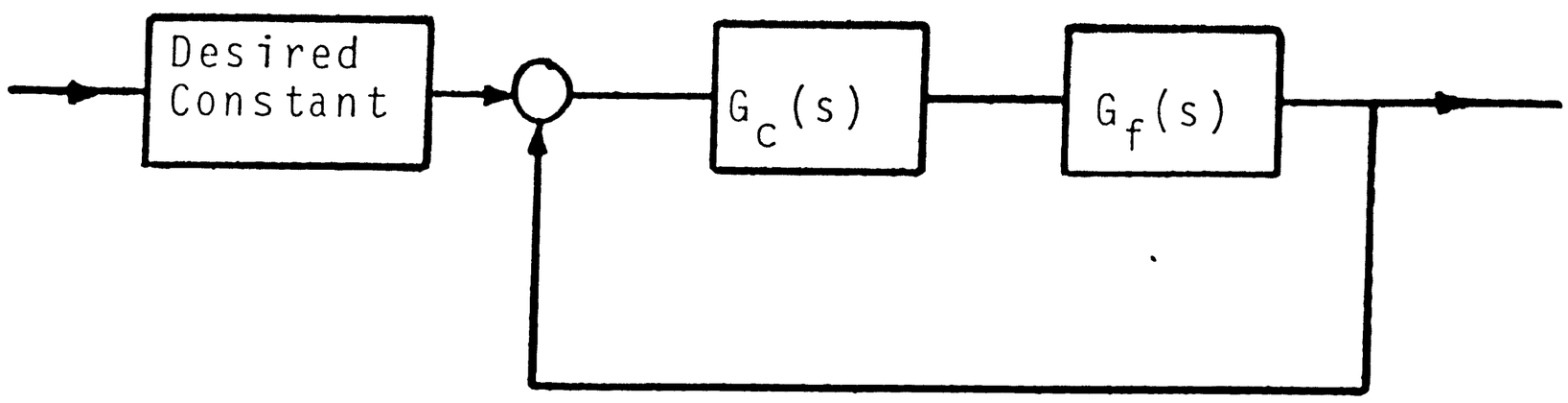

(b) Concept of Unity Feedback with Forward Path Compensator

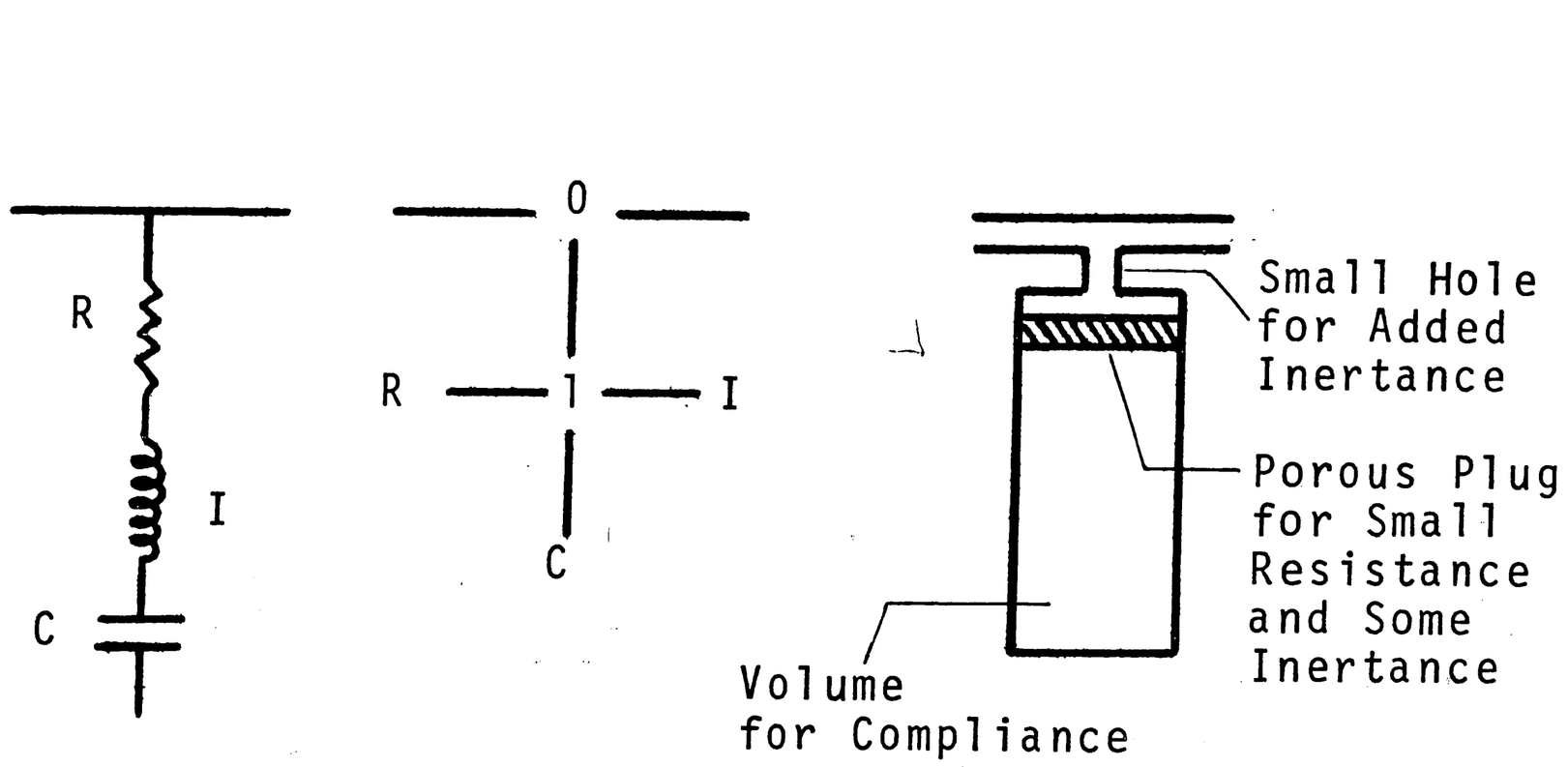

(c) Concept for Passive Shunt Compensator

Figure 7. Concept of Modified Optimal Control

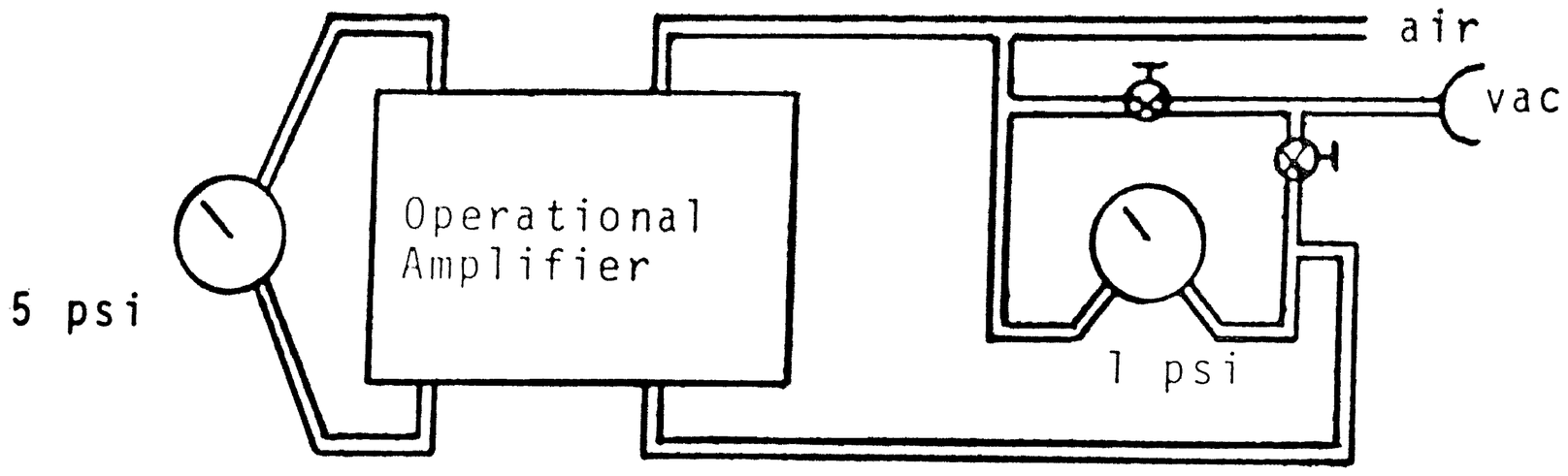

Figure 8. Schematic for Static Gain Test.

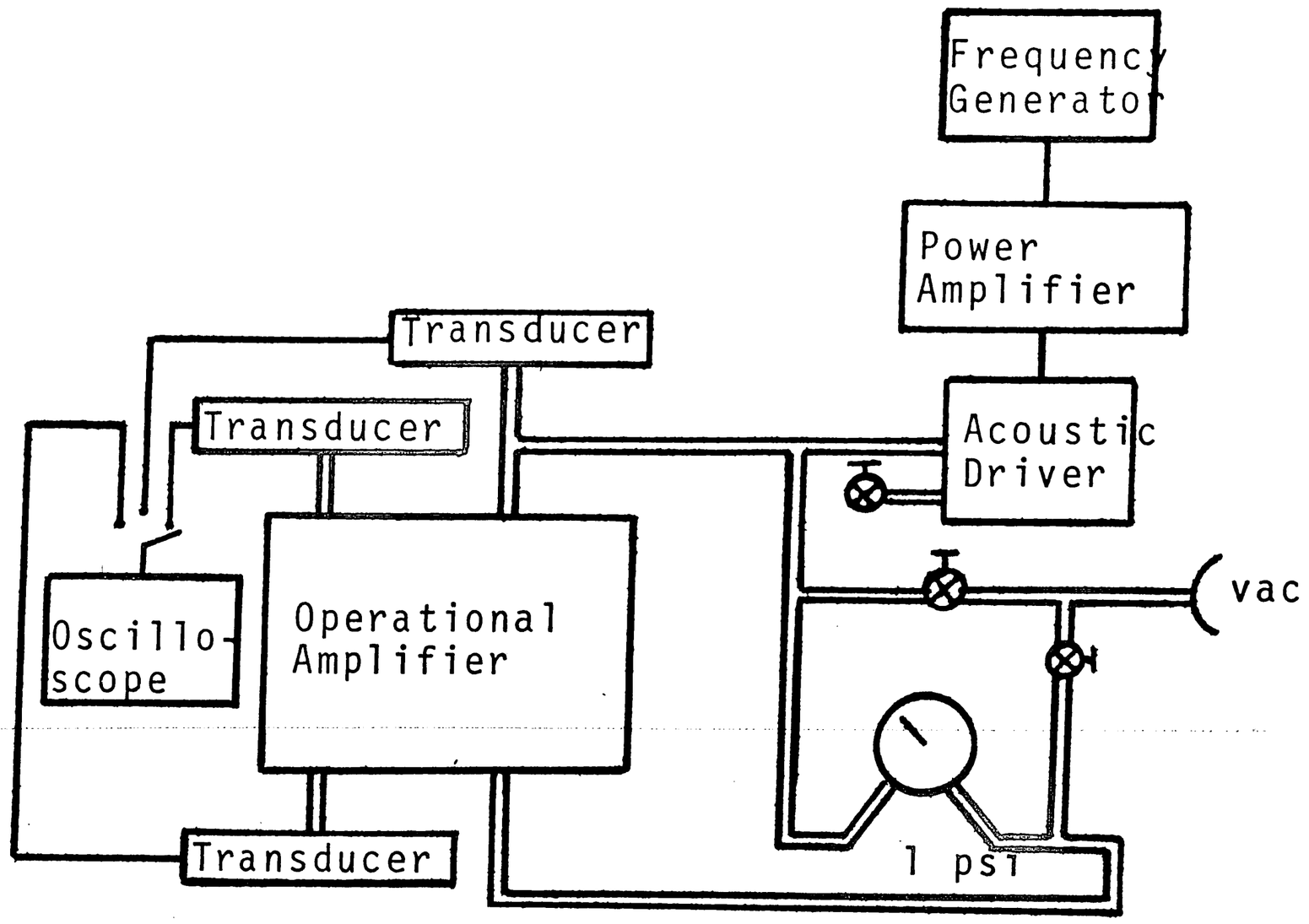

Figure 9. Schematic for Frequency Response Tests.

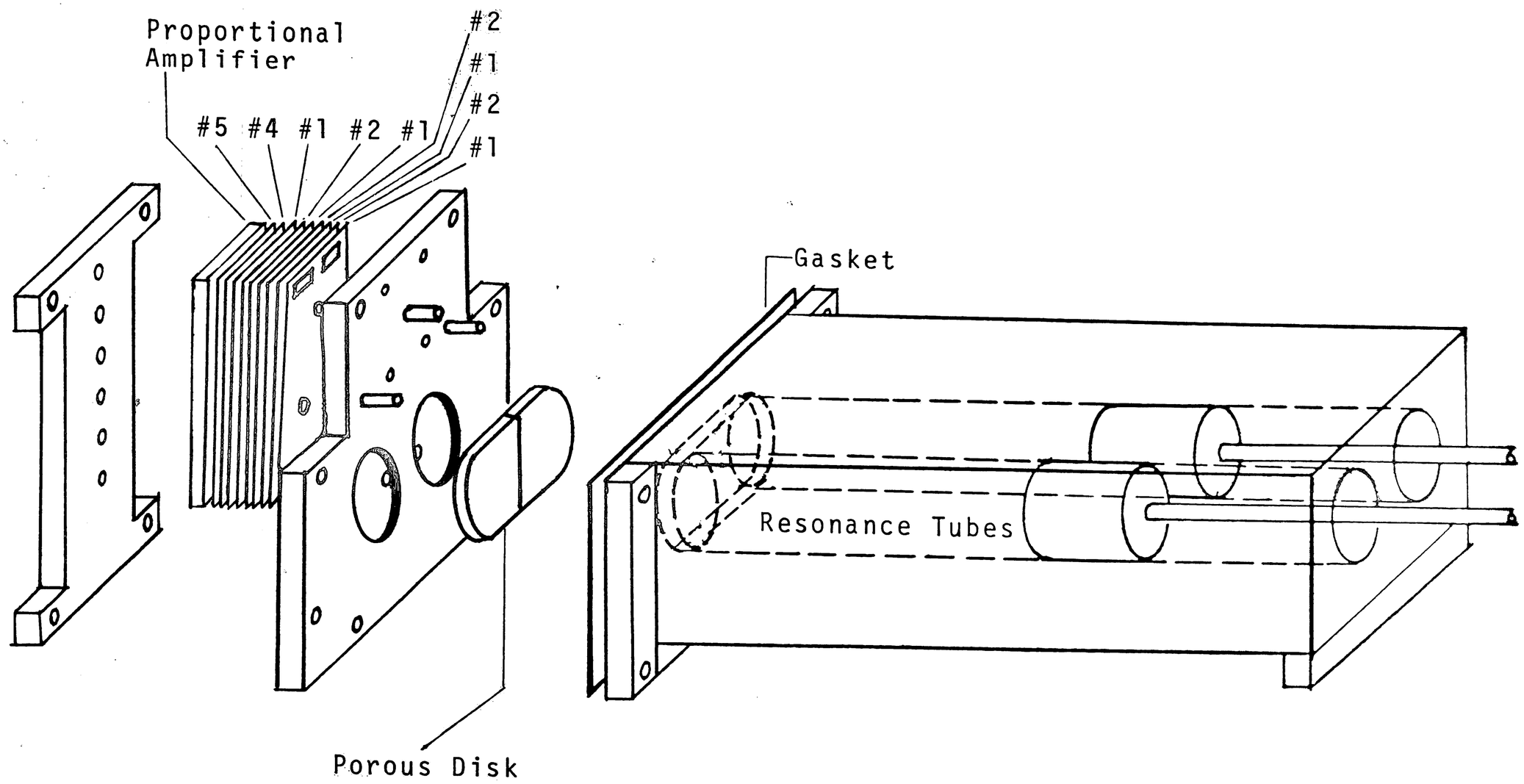

Figure 10. Exploded View of Apparatus.

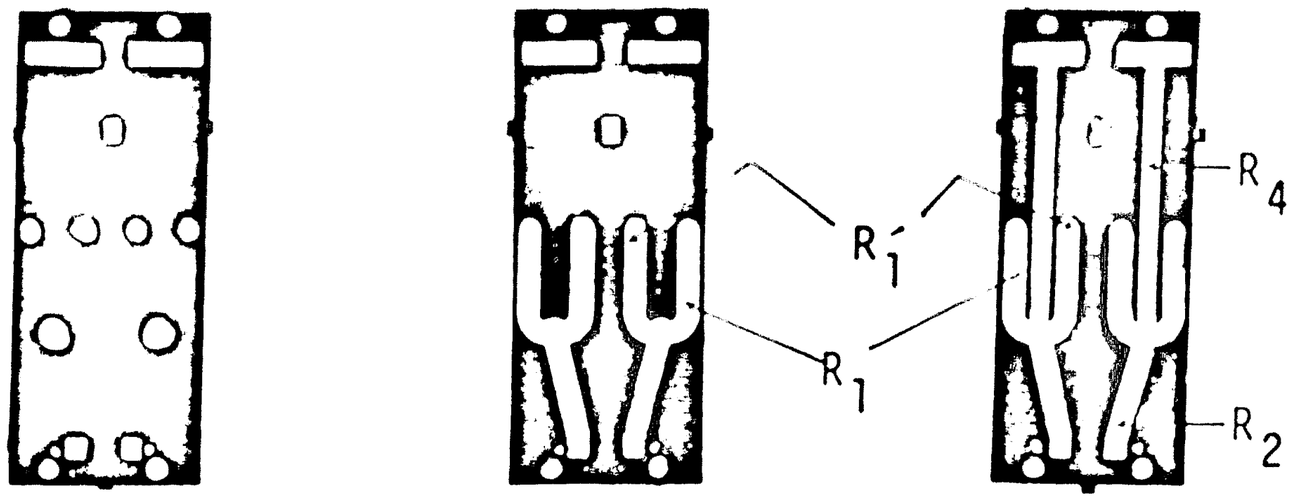

#1 #2 #3

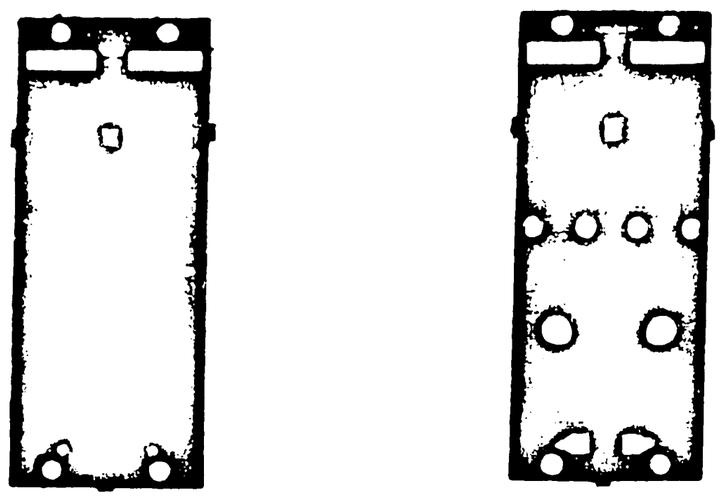

#4 #5

Figure 11. Resistances R_1, R_1', R_2 and R_4 Etched in Copper Berrylium Plates.

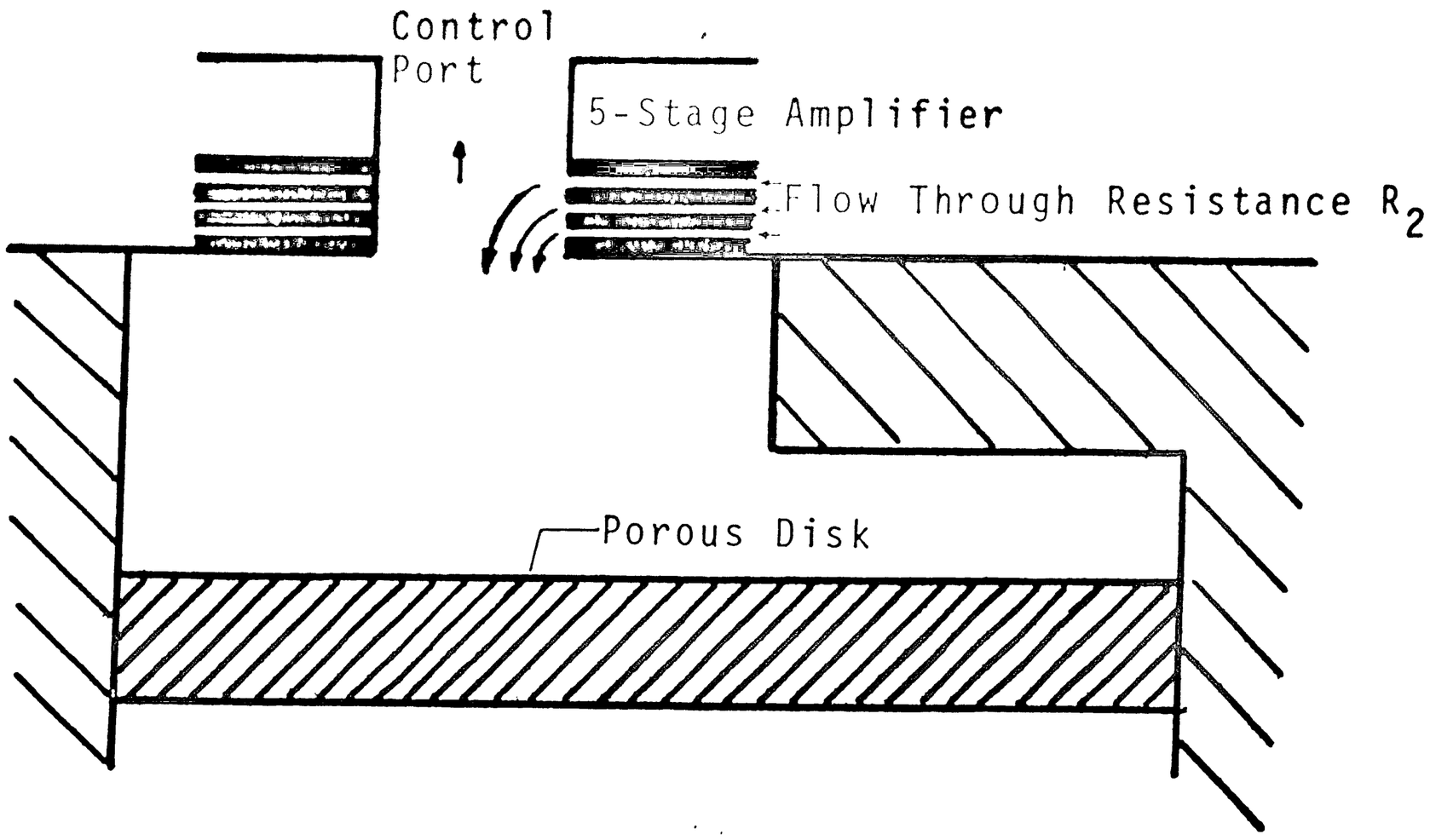

(a) Original Design

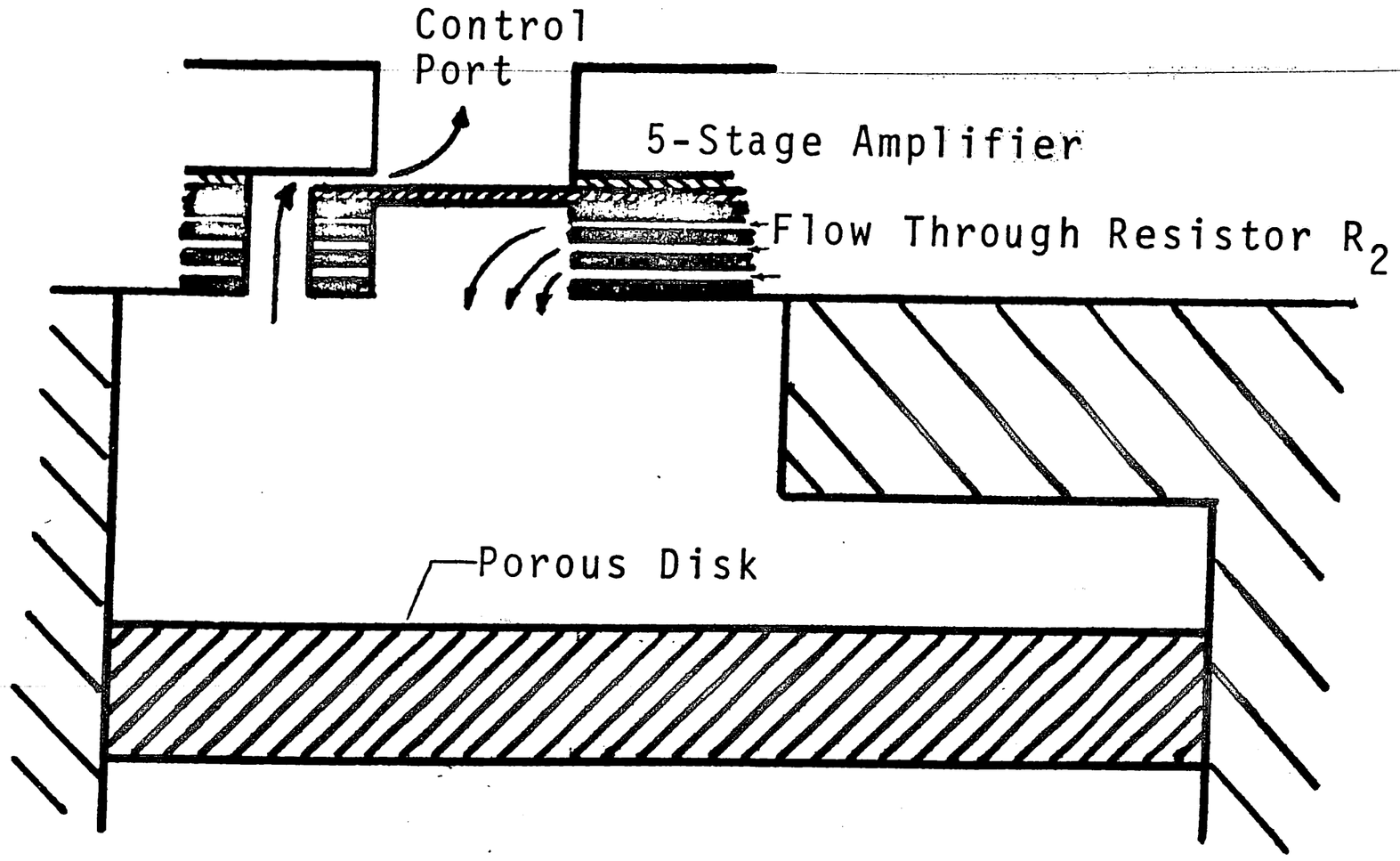

(b) Modified Design

Figure 12. Isolation of Control Port From Dynamic Head Effects of Flow Through R_2.

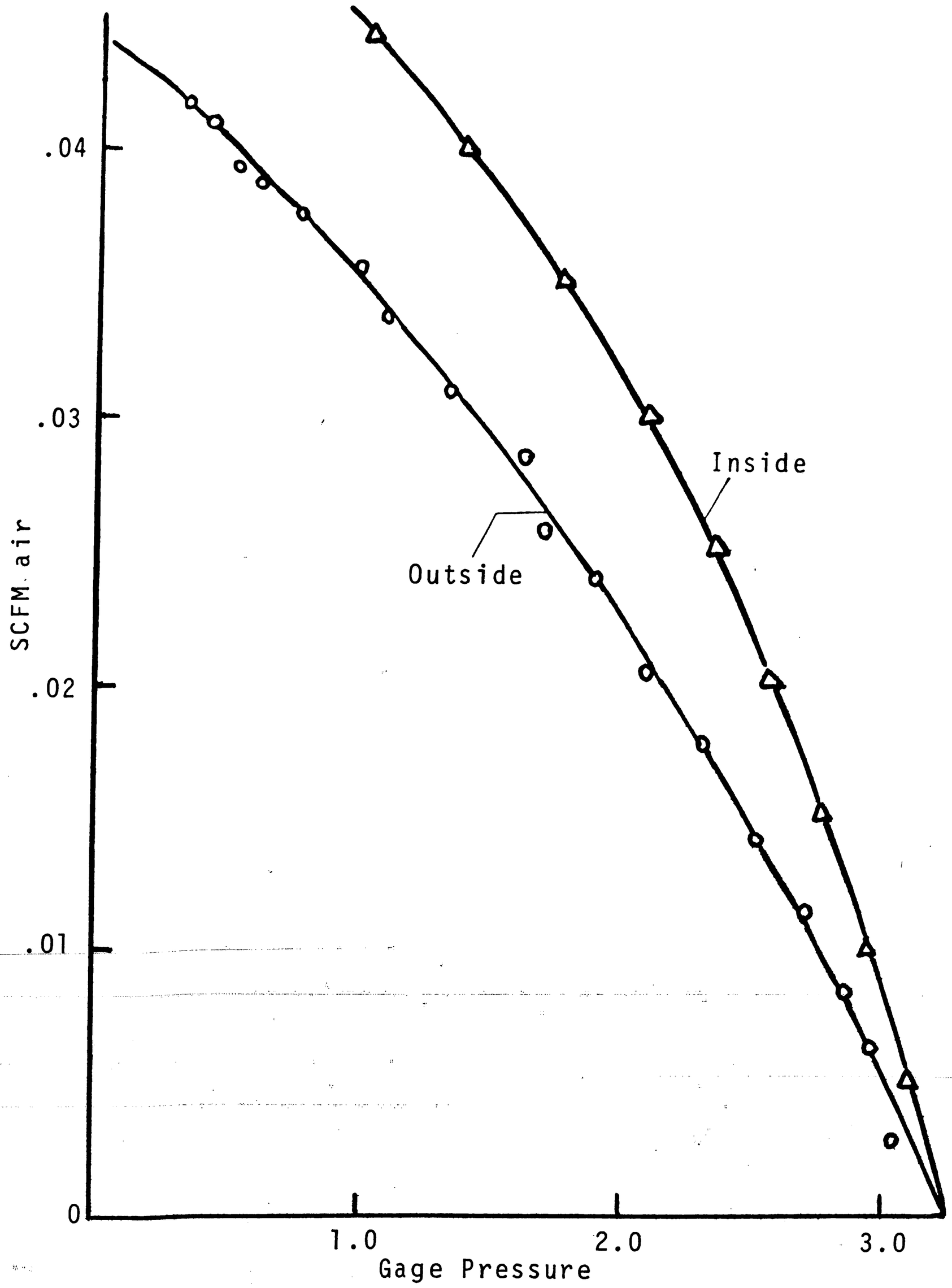

Figure 13. Output Pressure Flow Characteristics of Five-Stage Amplifier

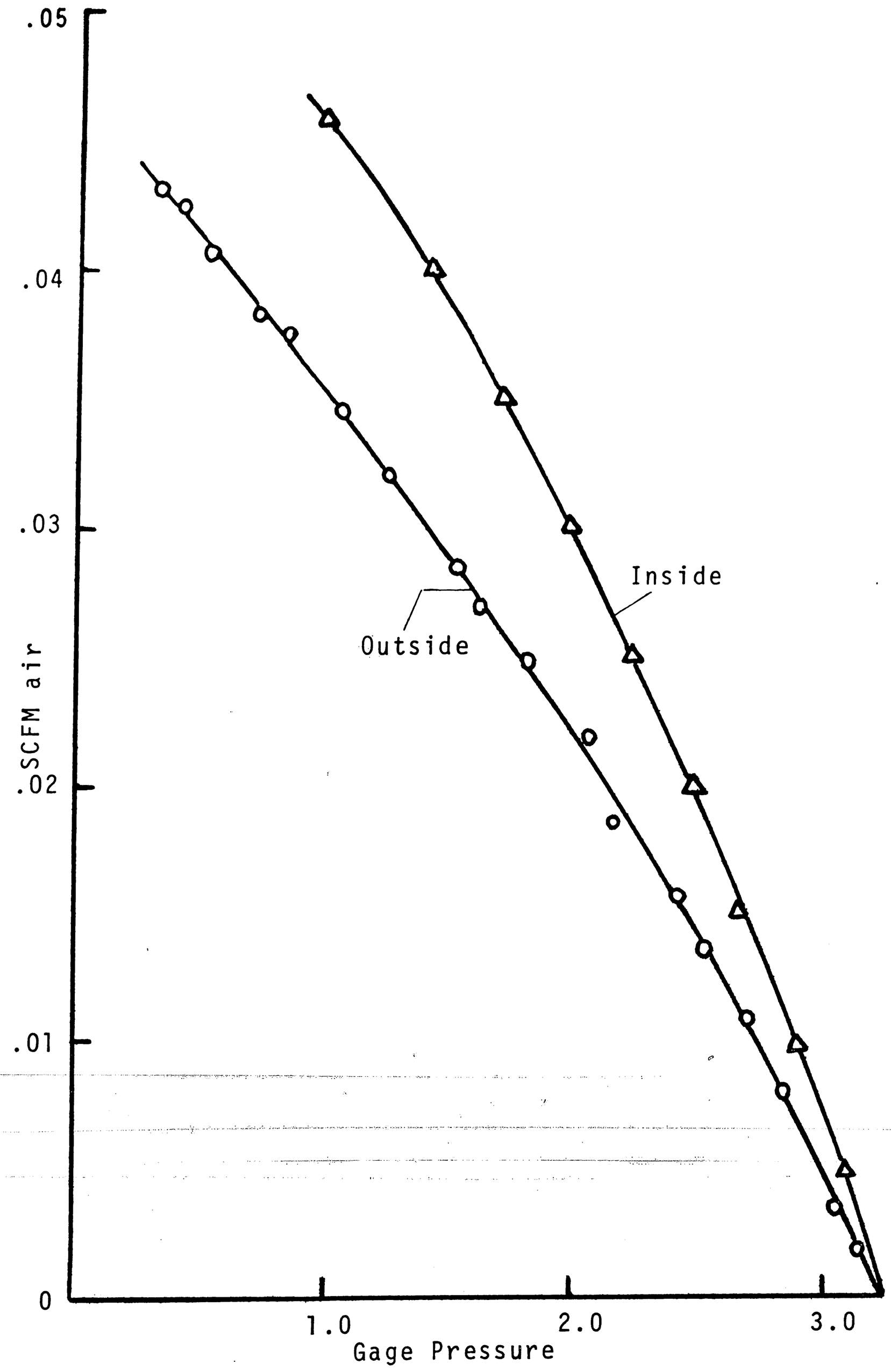

Figure 14. Output Pressure Flow Characteristics of Five-Stage Amplifier

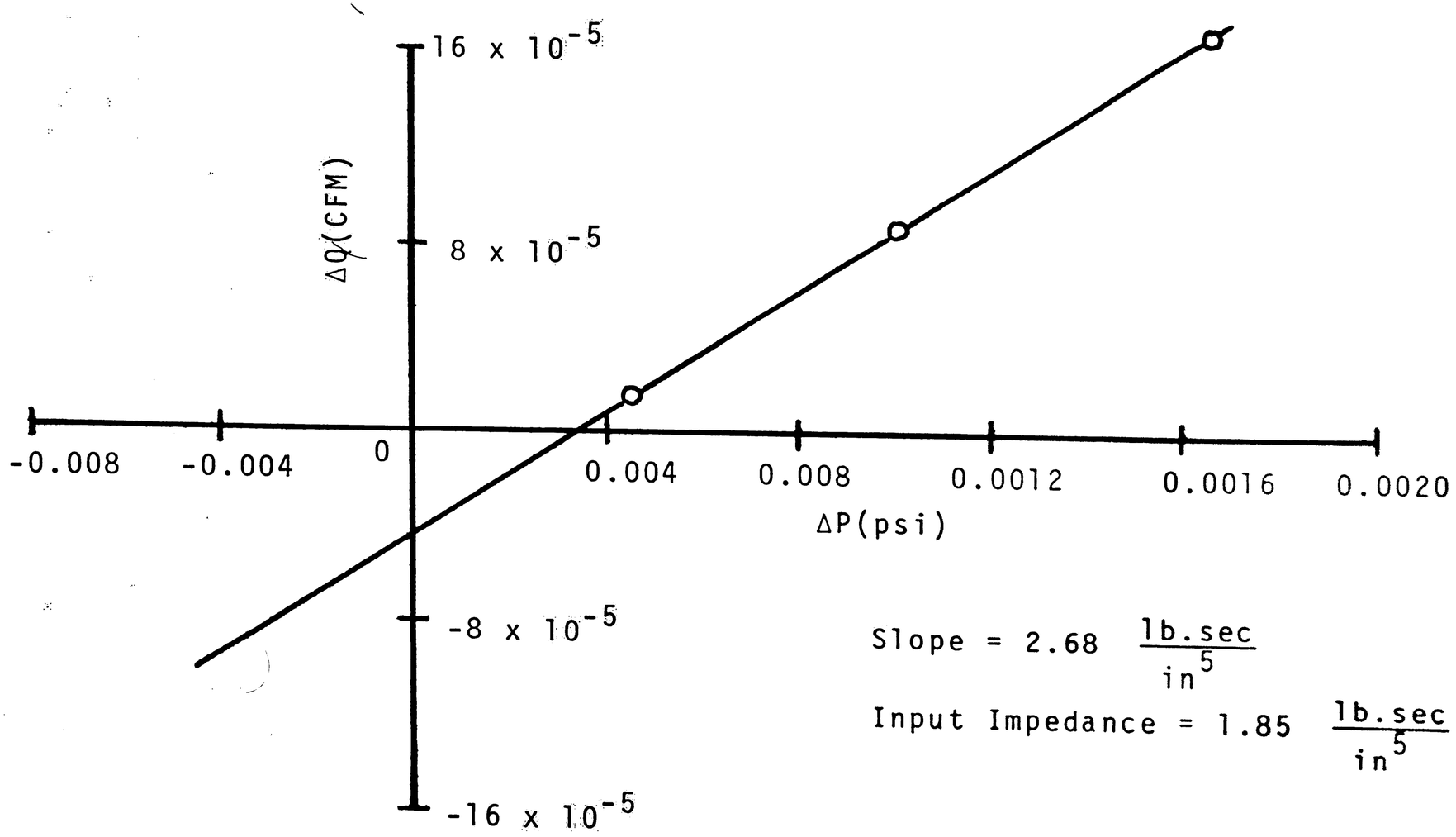

Slope = 2.68 $\frac{lb.sec}{in^5}$

Input Impedance = 1.85 $\frac{lb.sec}{in^5}$

Figure 15. Steady State Input Impedance of the Five-Stage Amplifier

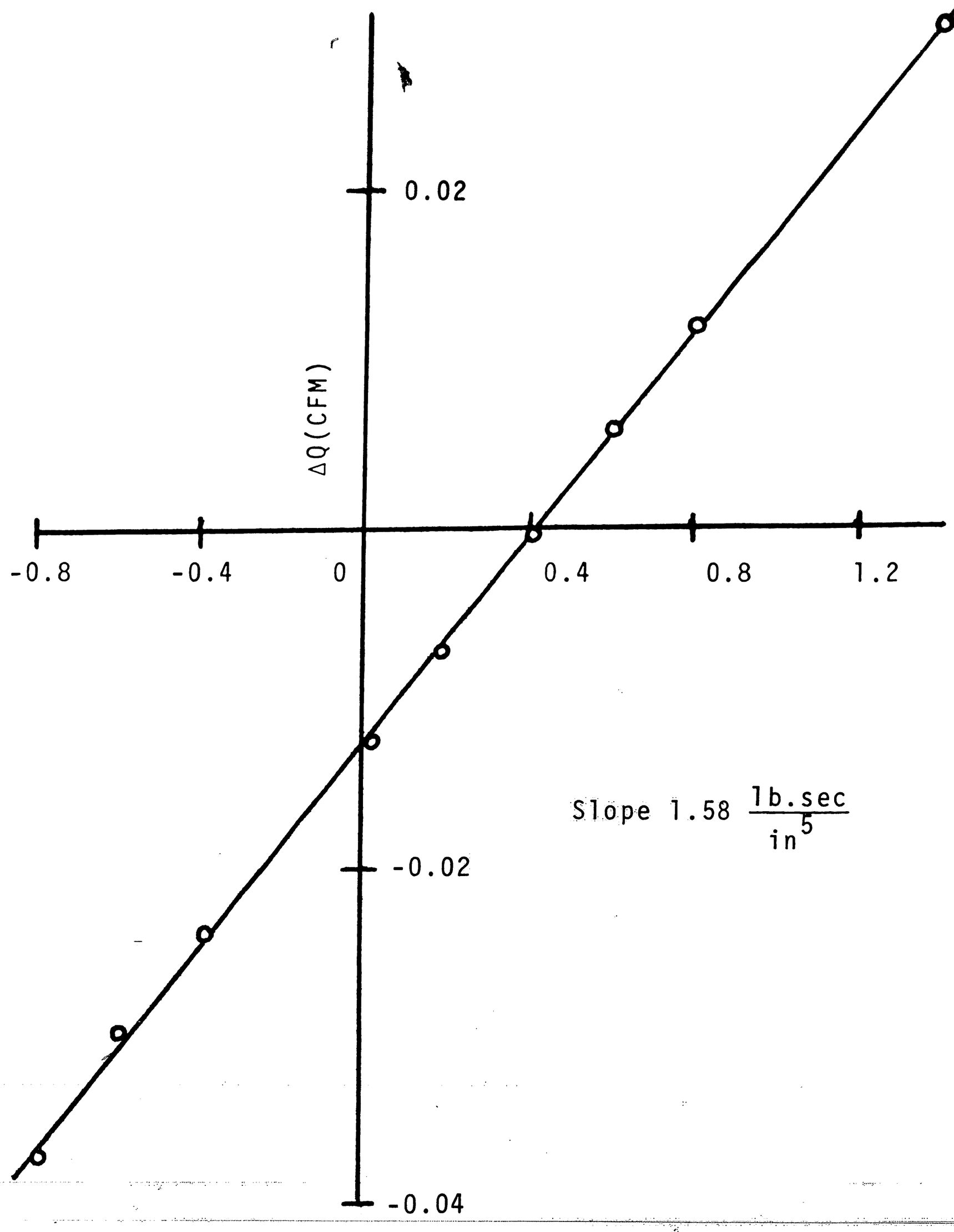

Figure 16. Steady-State Output Impedance of the Five-Stage Amplifier

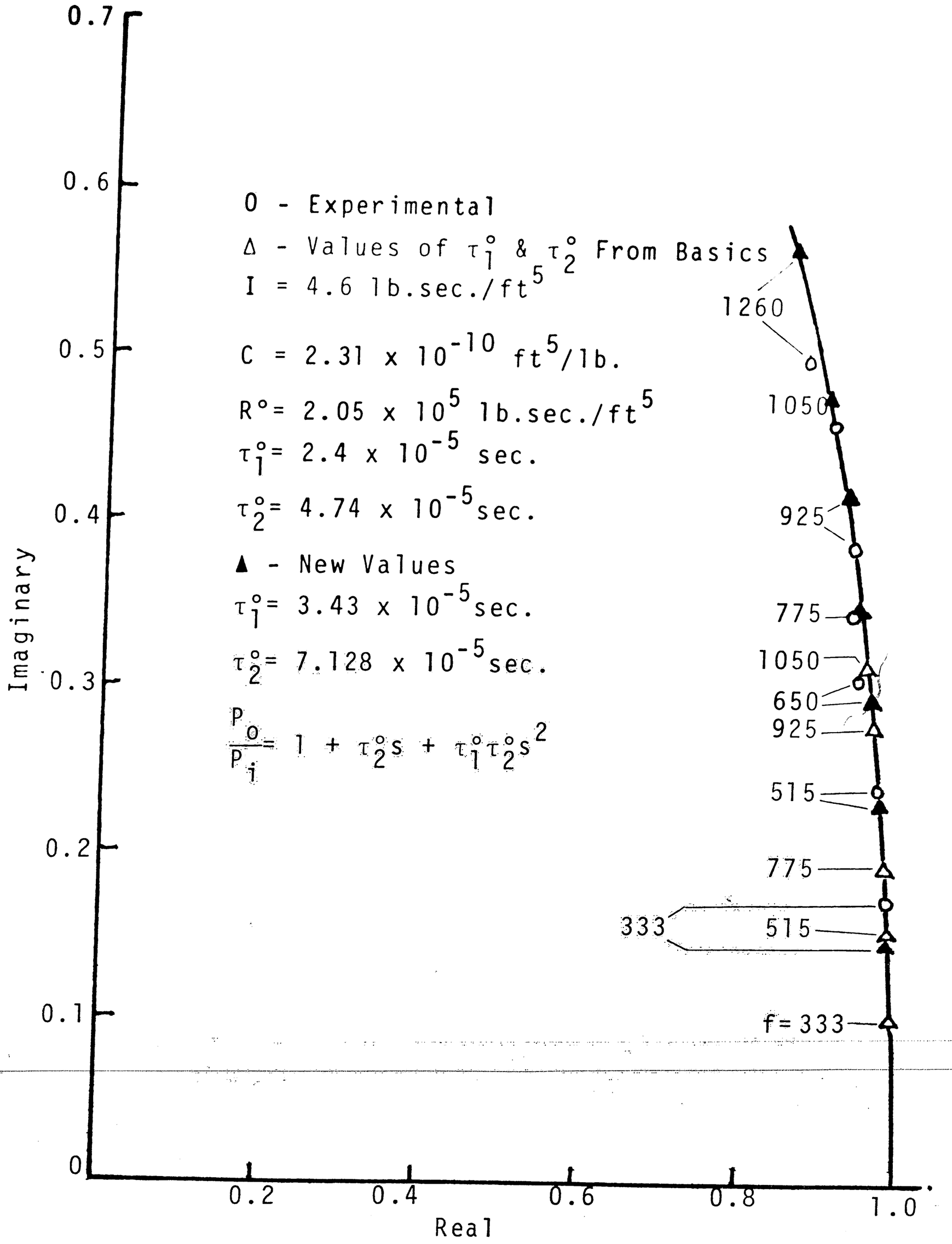

Figure 17. P_o/P_i at the Control Ports (when $Y_i = 0$).

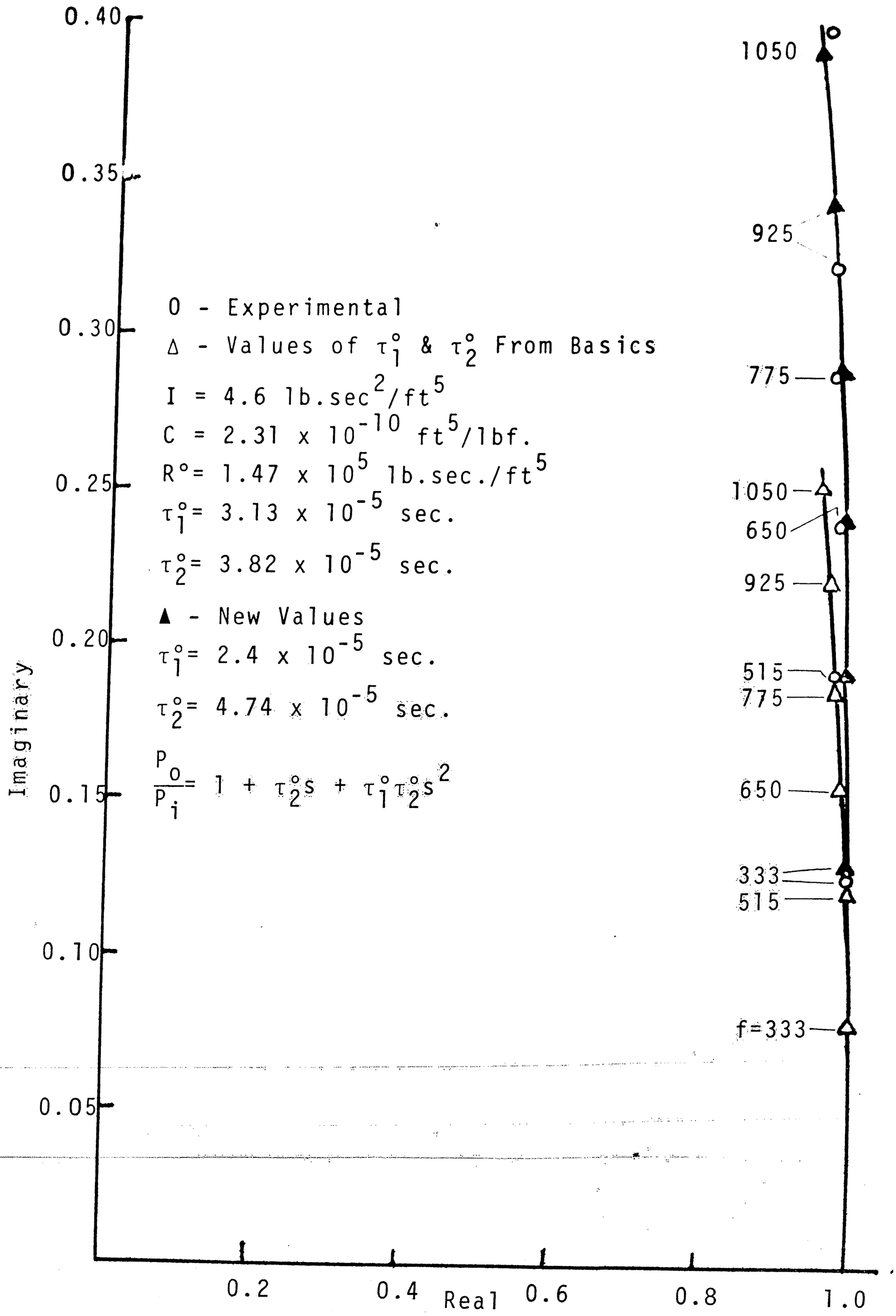

Figure 18. P_o/P_i at Output Ports (when $1/Z_o = 0$).

$$R_o = 0.785 \frac{lb.sec}{in^5}$$

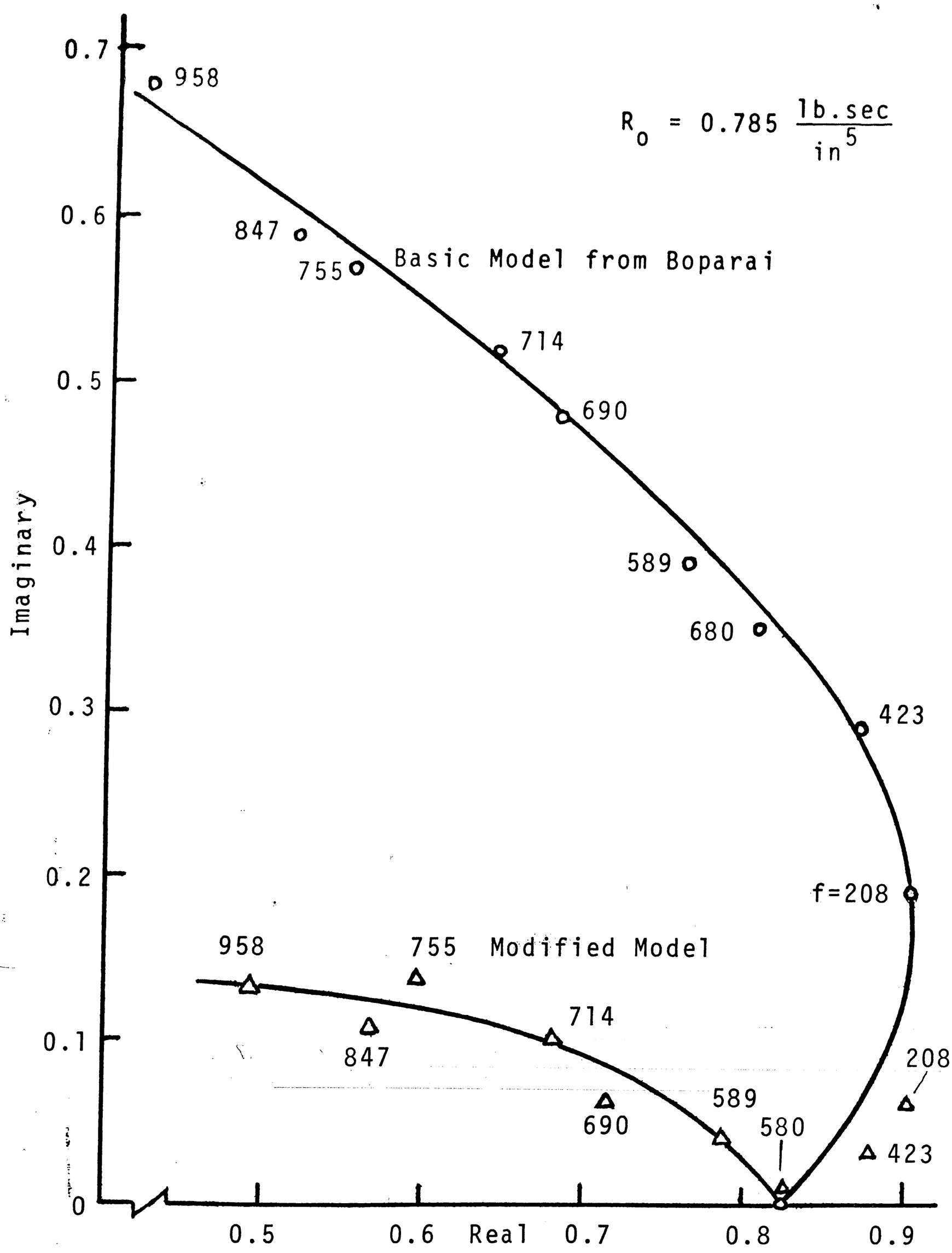

Figure 19. Dimensionless Output Admittance of the Proportional Amplifier. R_o/Z_o

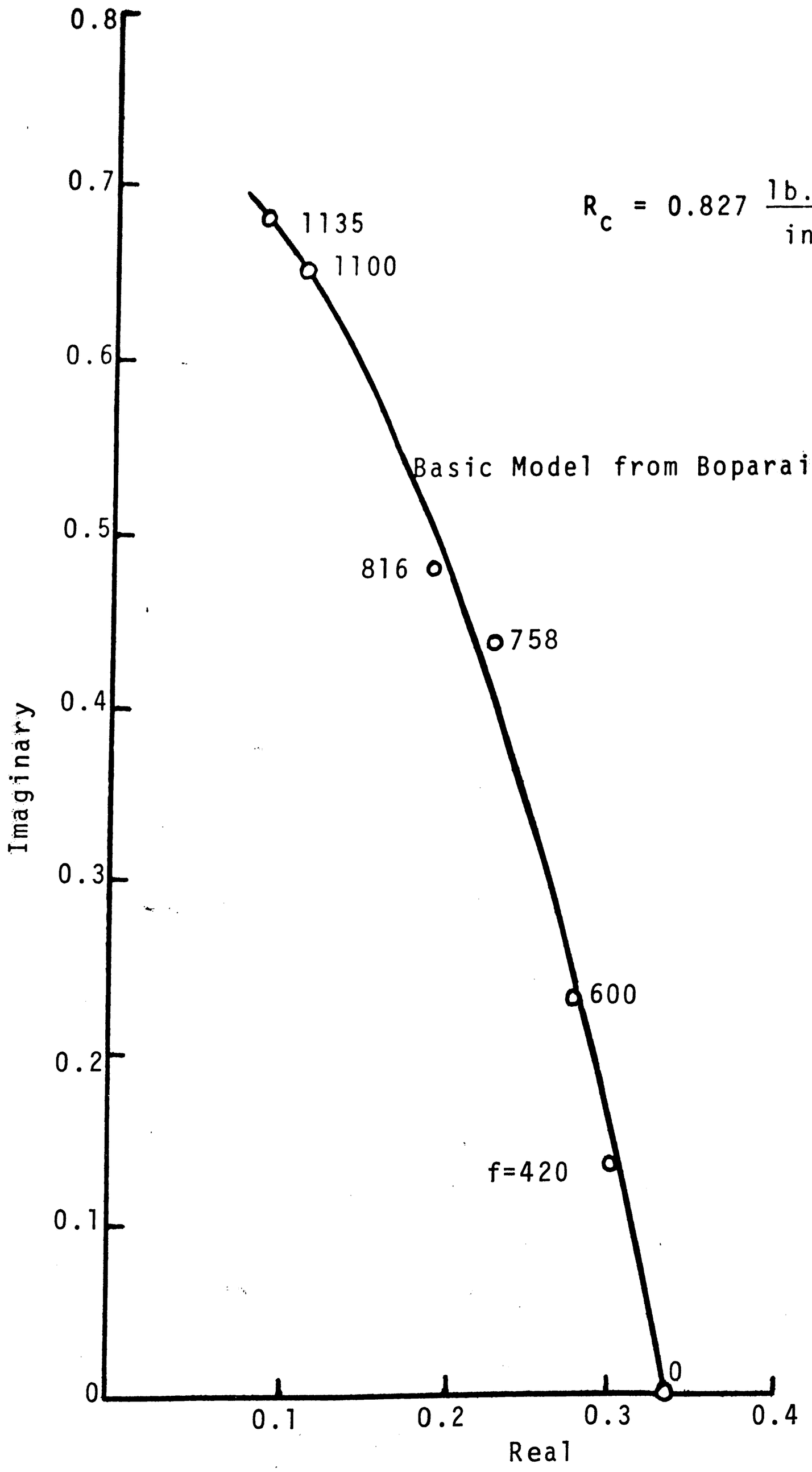

Figure 20. Dimensionless Input Admittance of the Proportional Amplifier $Y_i R_c$.

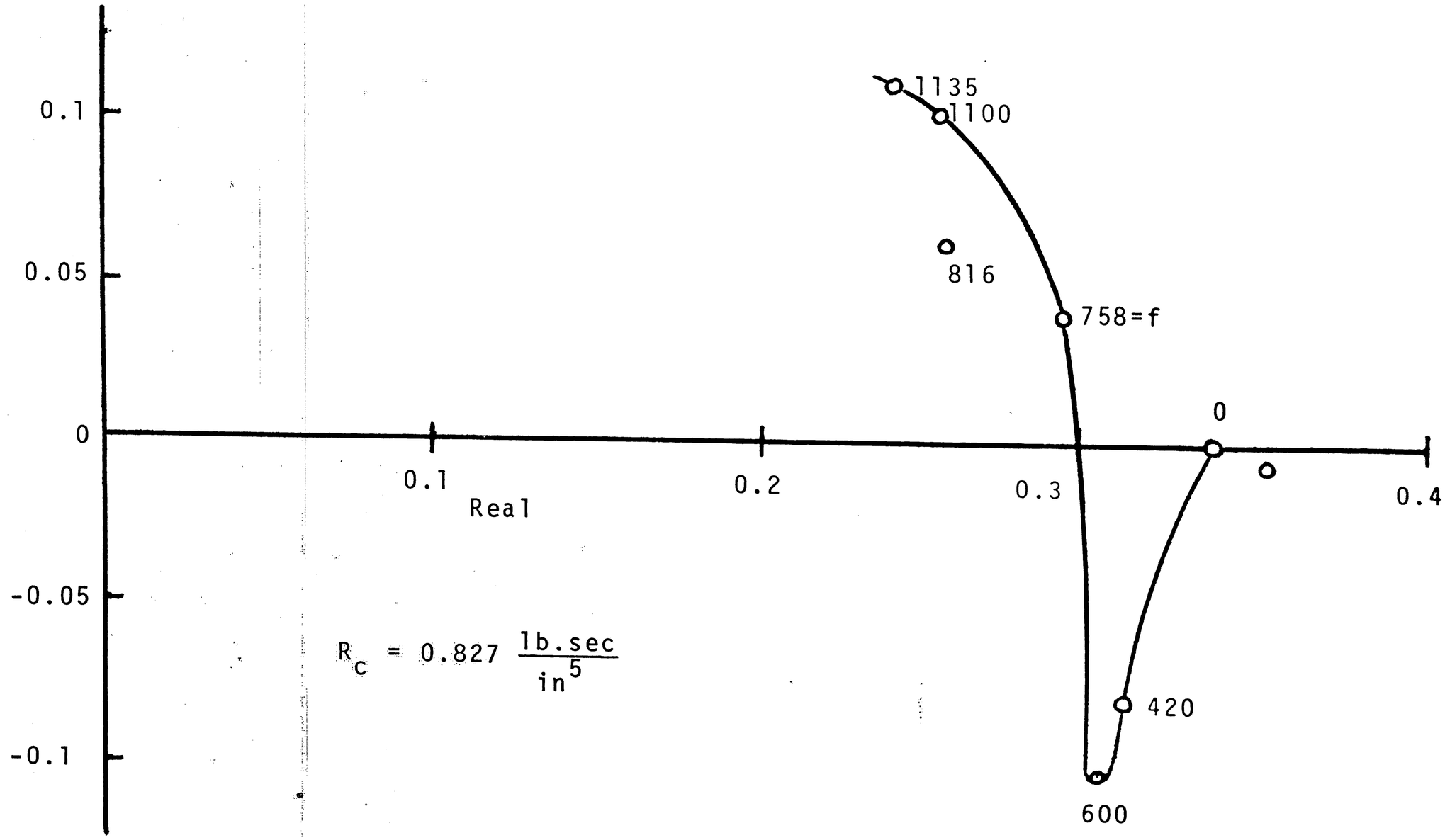

$R_c = 0.827 \frac{lb.sec}{in^5}$

Figure 21. Modified Input Admittance of the Proportional Amplifier $Y_i R_c$.

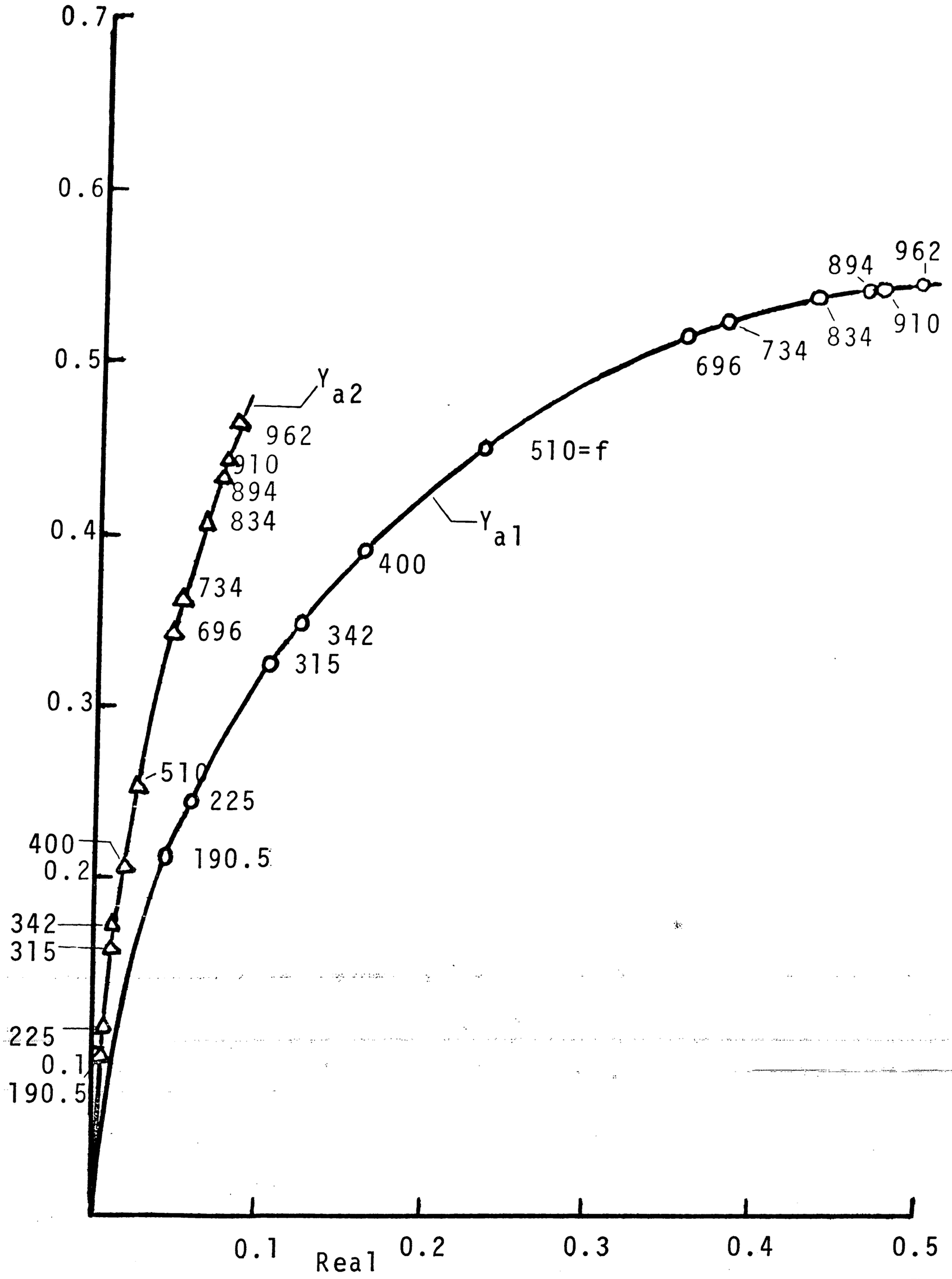

Figure 22. Admittance of the Actual Load $Y_a \times 10^5 \frac{ft^5}{lb.sec}$

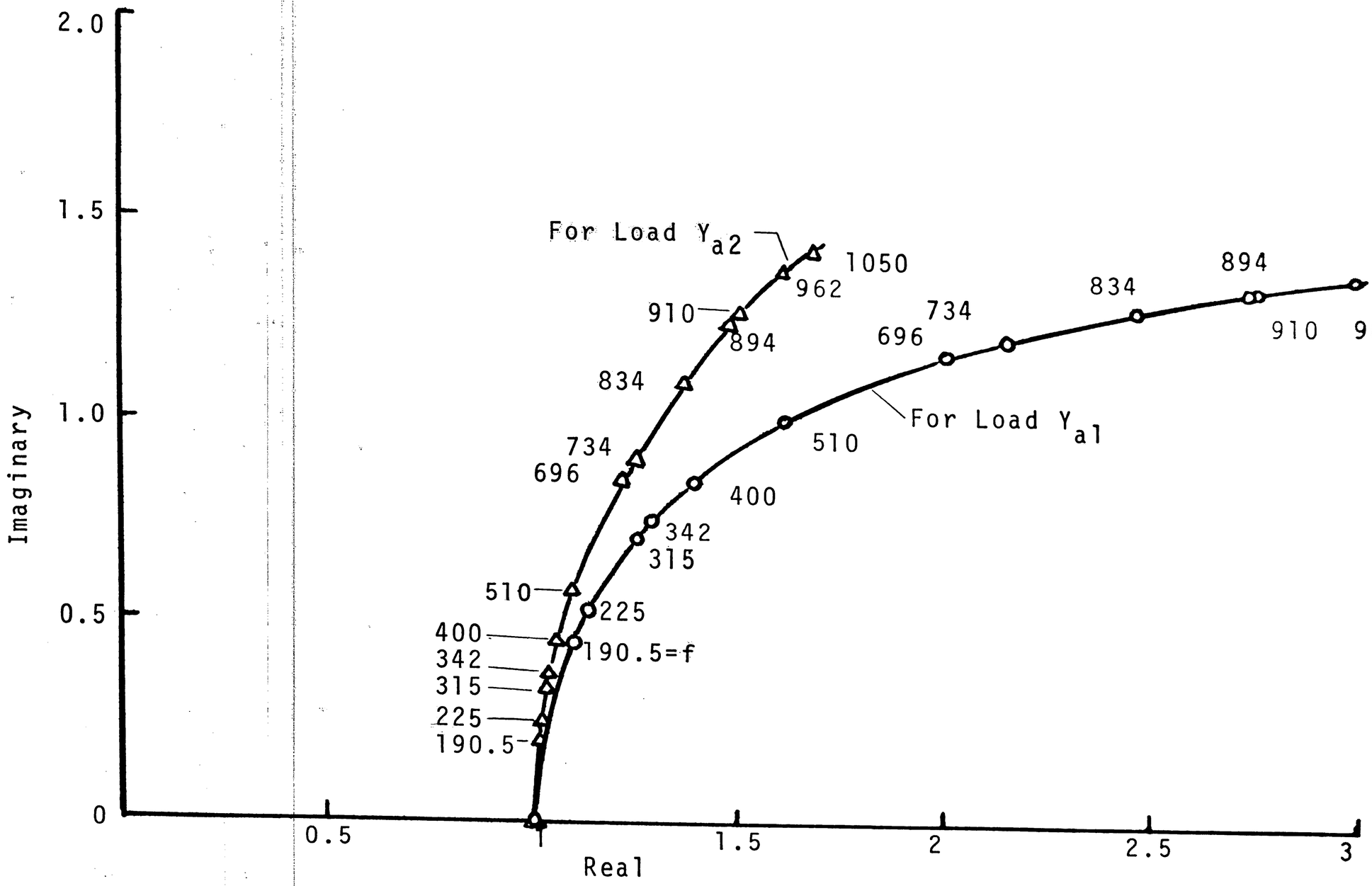

Figure 23. Modification Factor for the Transfer Characteristics. F

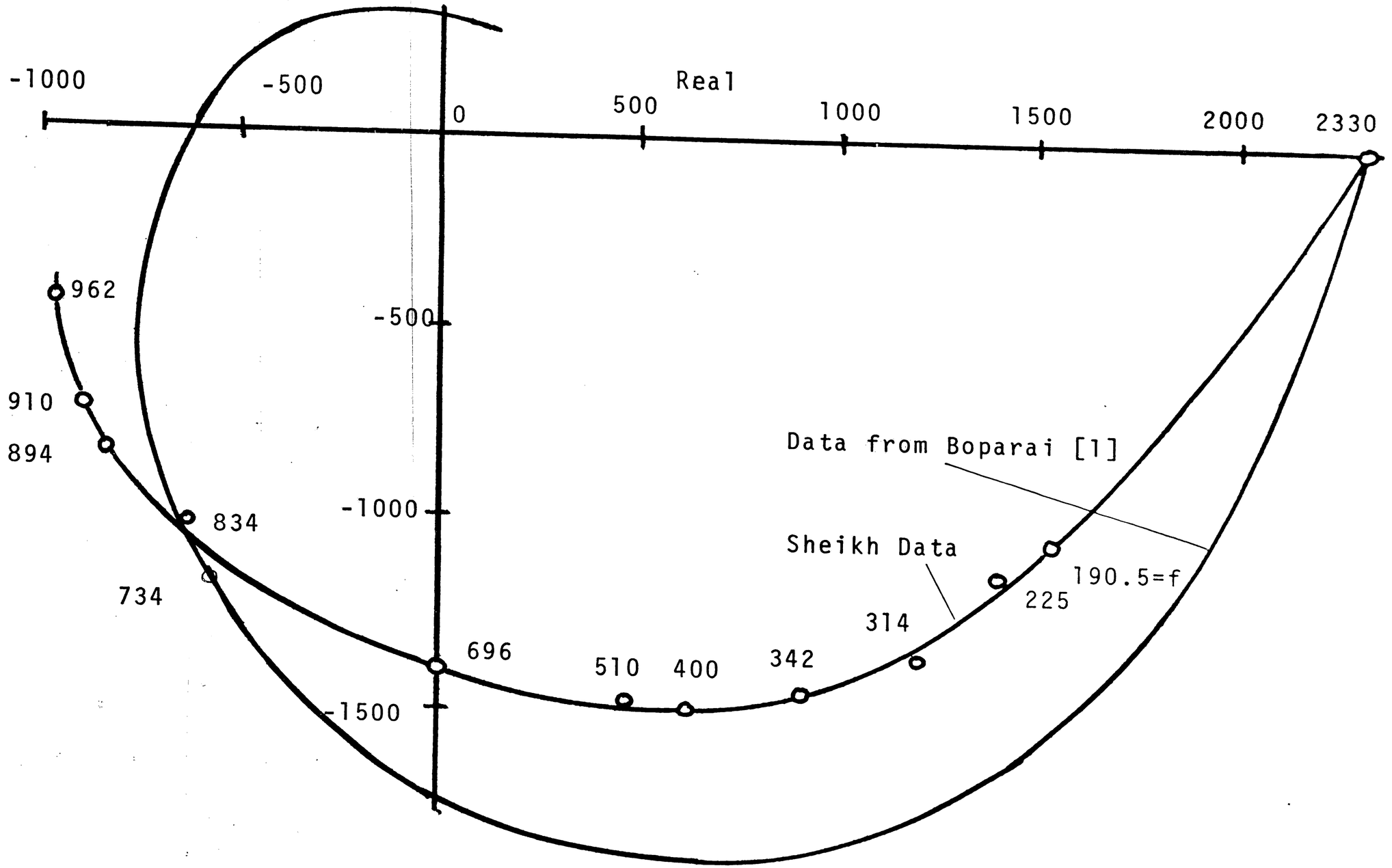

Figure 24. Transfer Characteristic (Uncorrected) with Load Y_{al}.

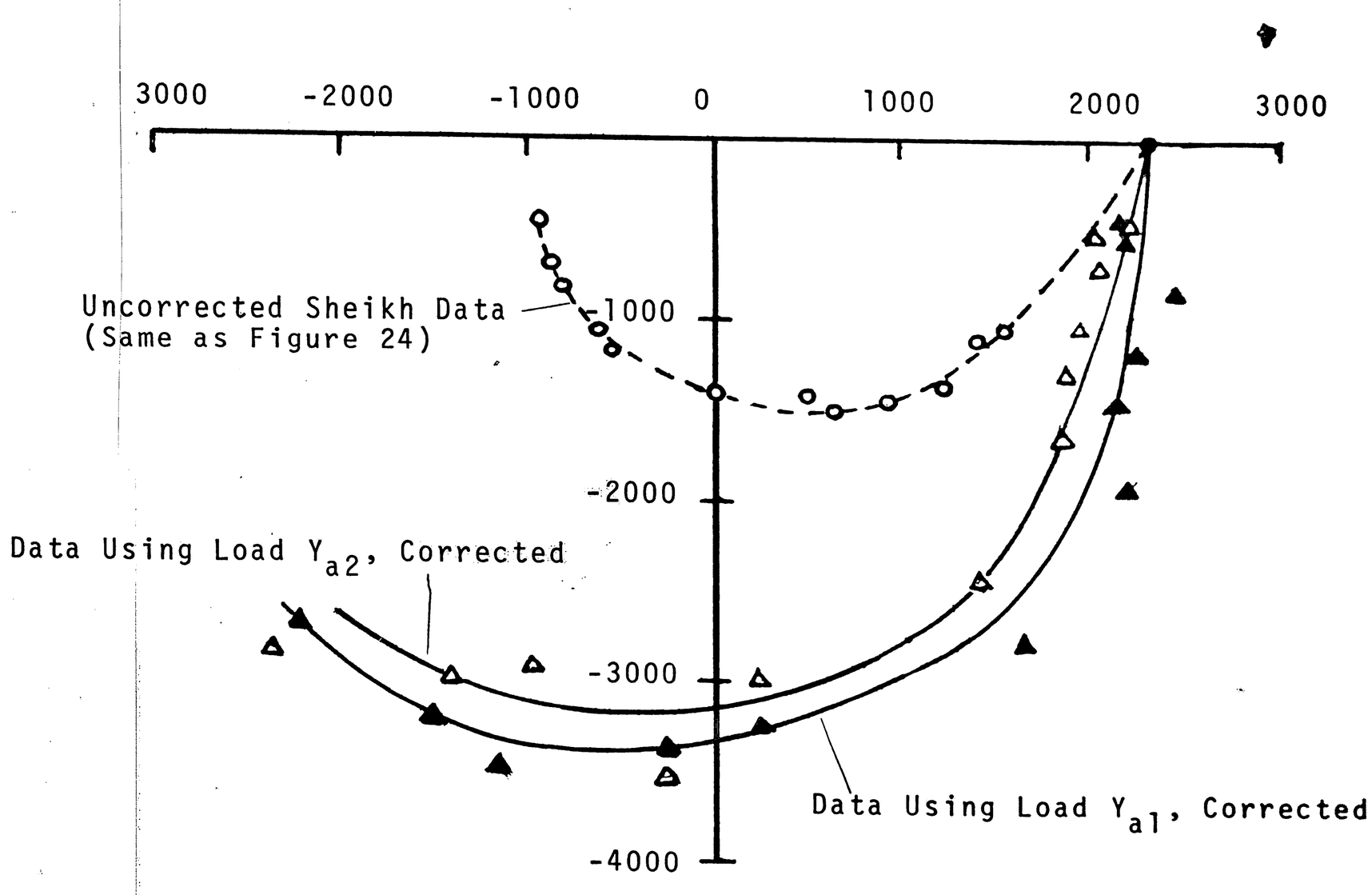

Figure 25. Corrected Transfer Characteristics.

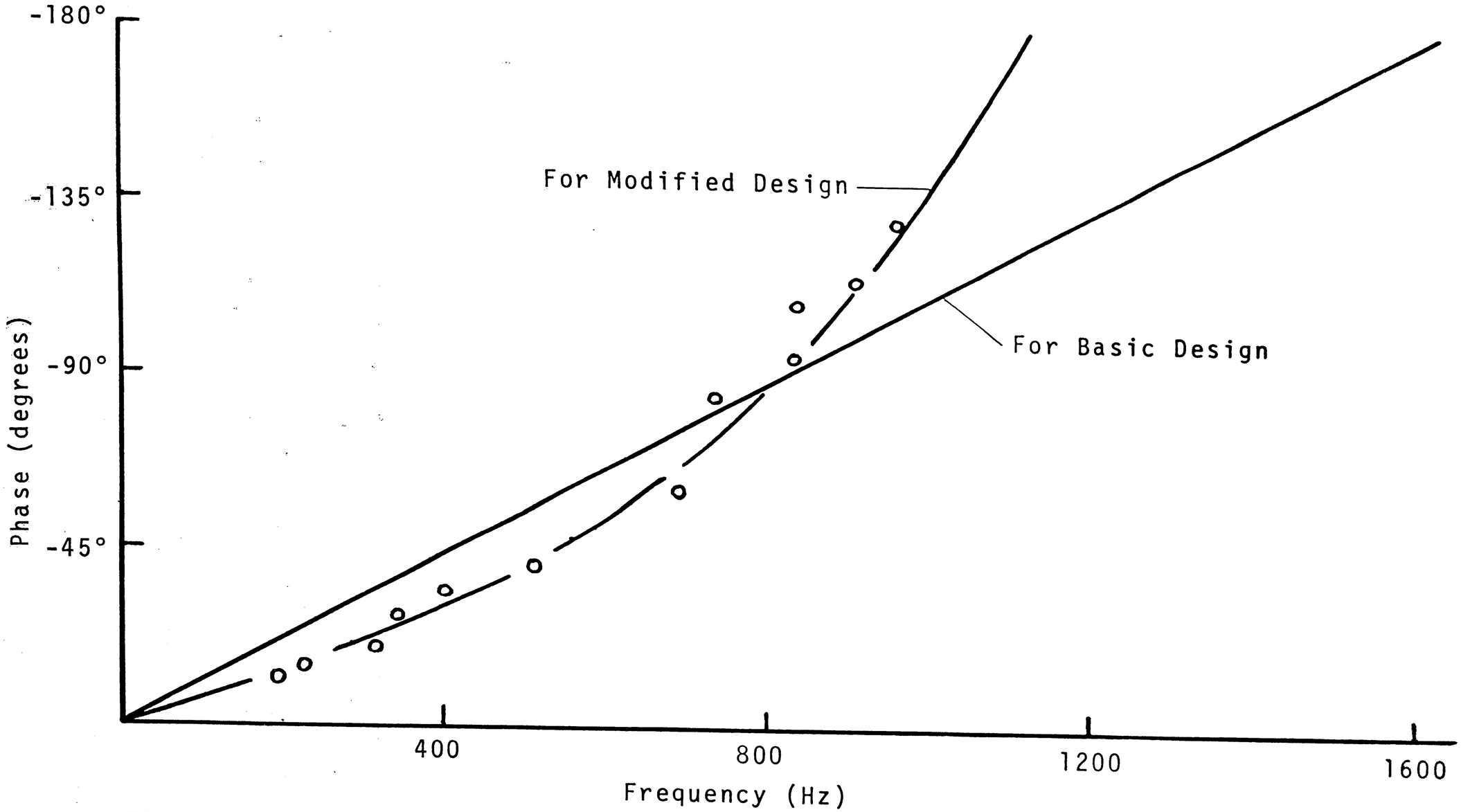

Figure 26. Phase vs. Frequency for the Gain of the Proportional Amplifier.

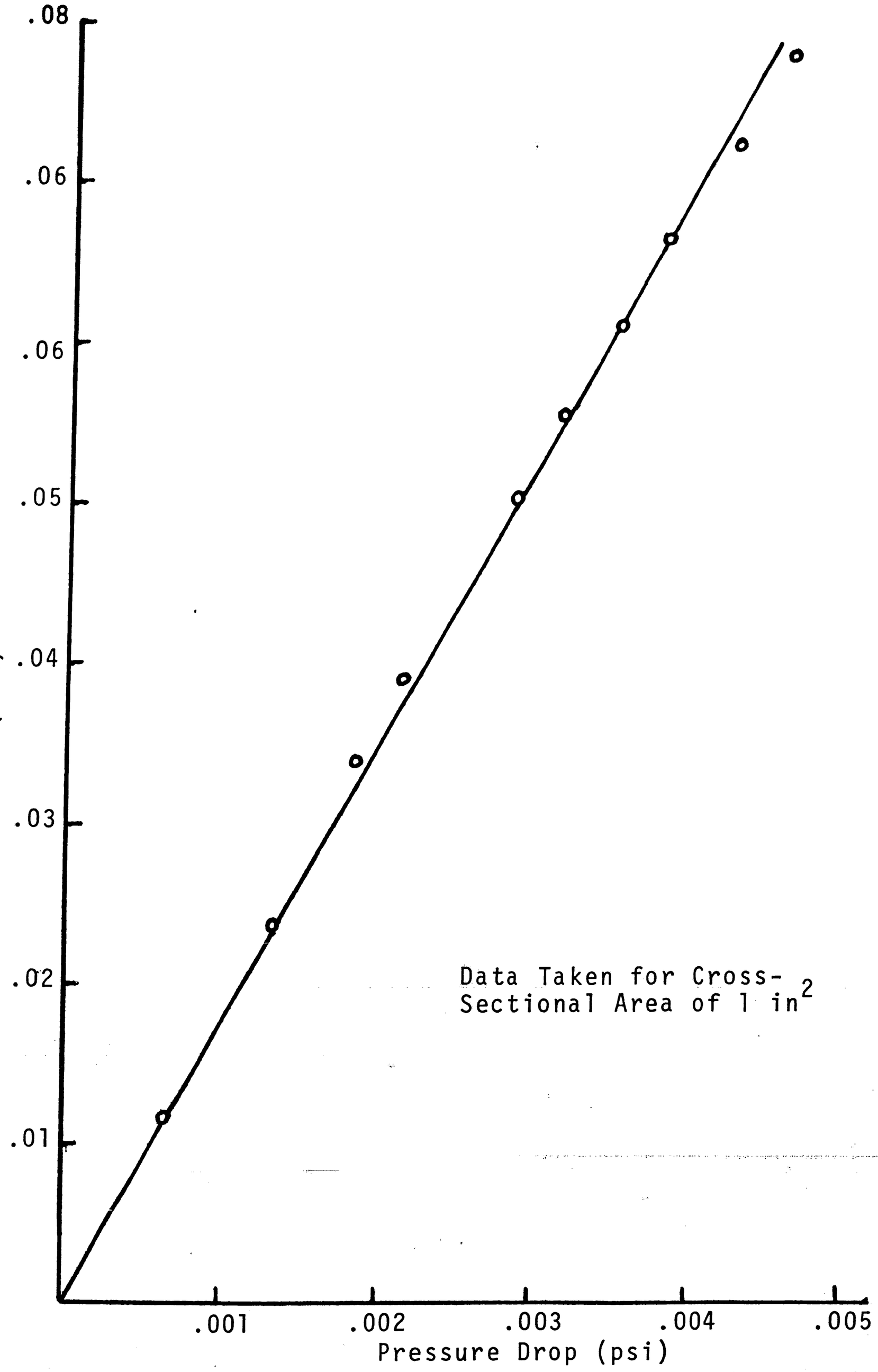

Figure 27. Resistance of Porous Disk.

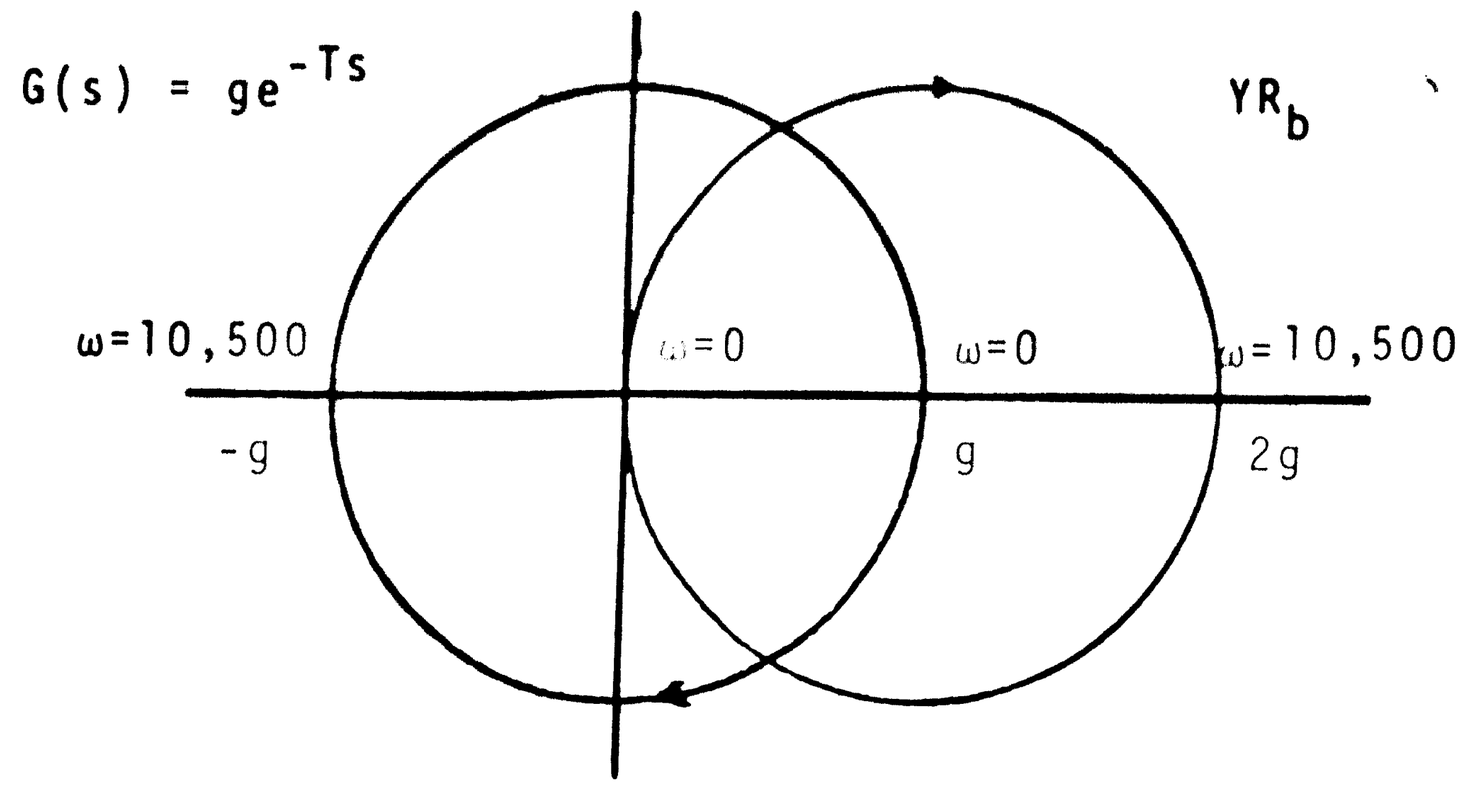

(a) Numerator and Denominator of Open Loop Gain

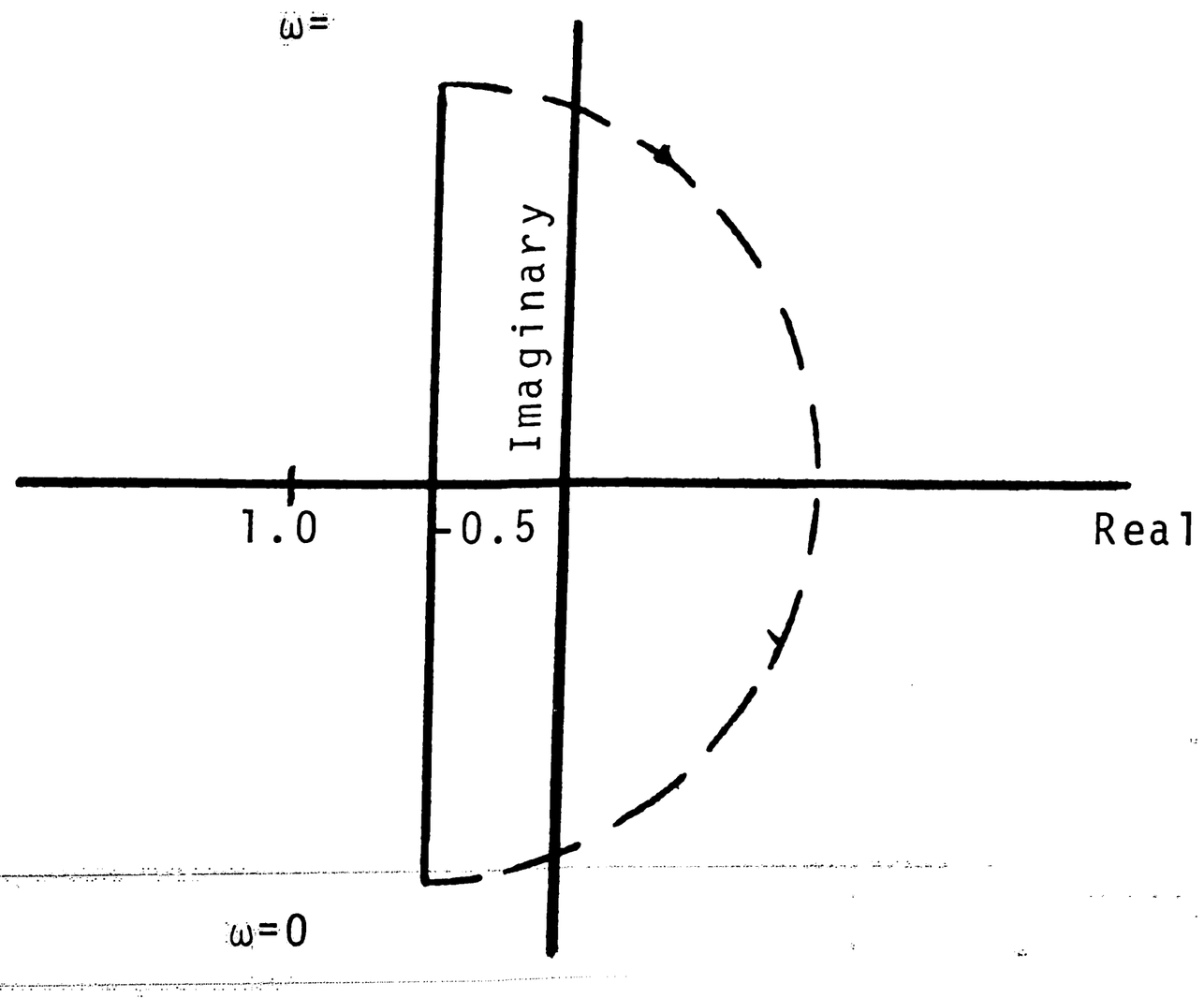

(b) Open Loop Gain

Figure 28. Nyquist Plot for Idealized Model of Operational Amplifier.

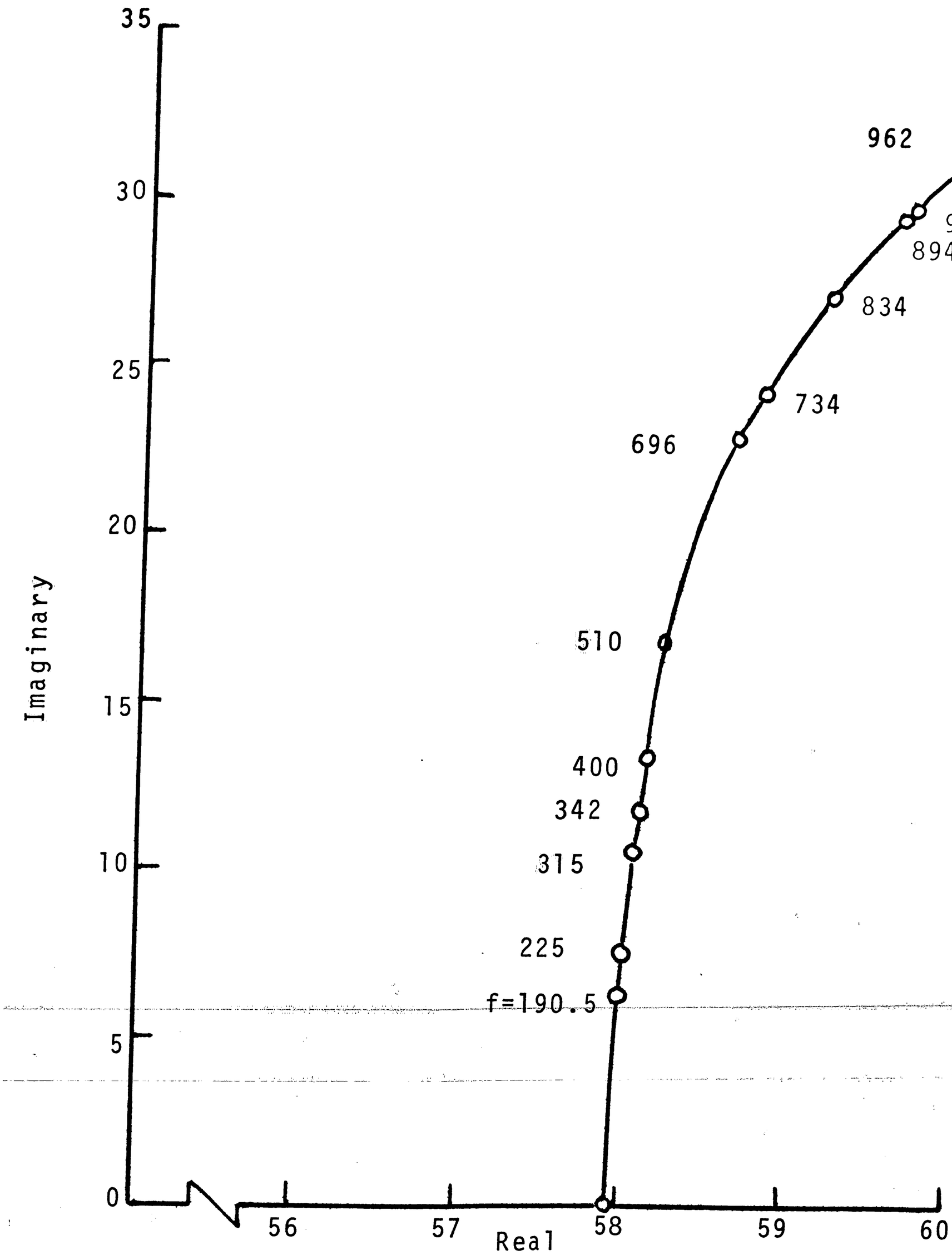

Figure 29. Nyquist Plot of R_b $\frac{lb.sec}{in^5}$

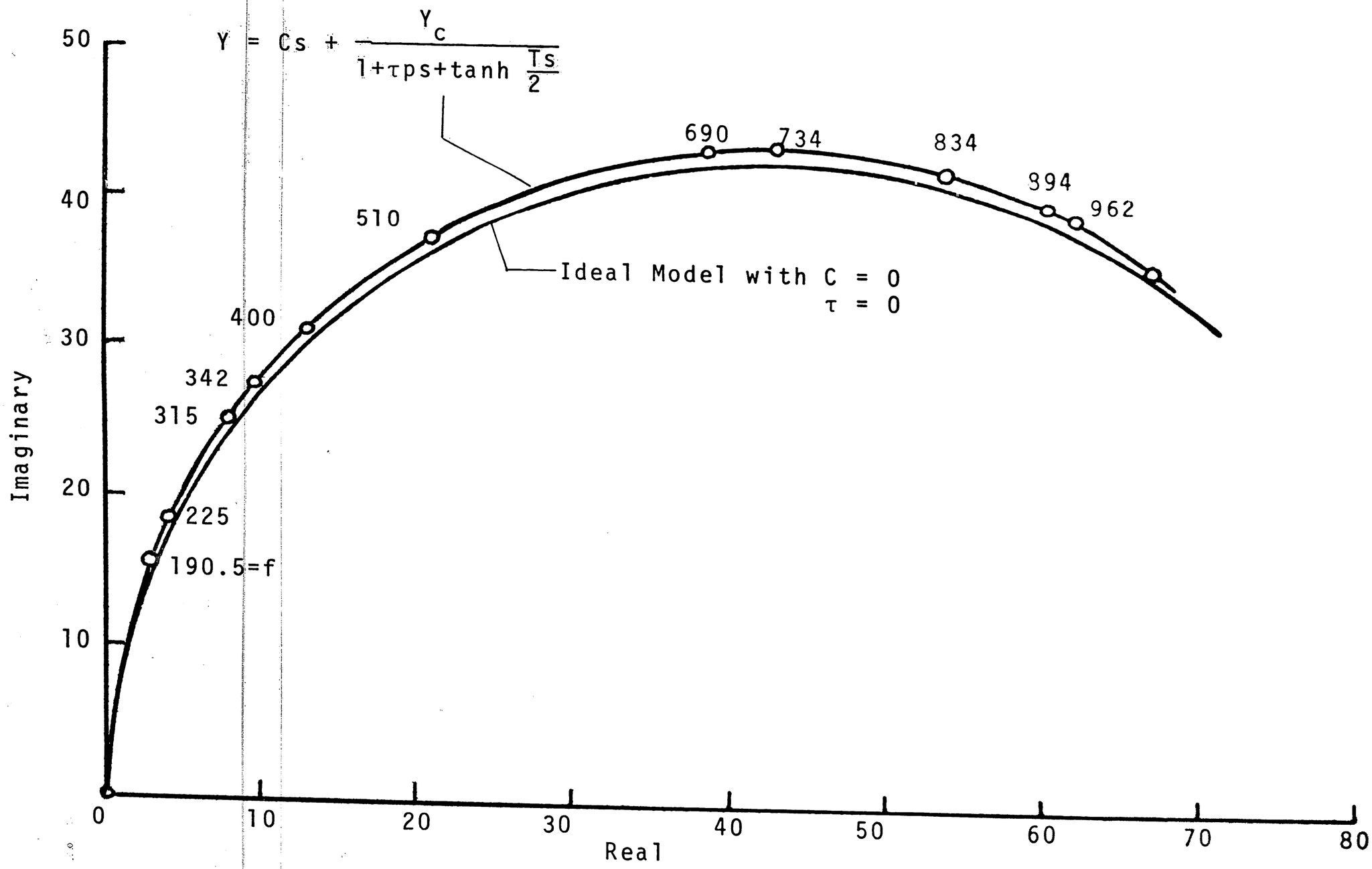

Figure 30. The Admittance Y $in^5/lb.sec.$

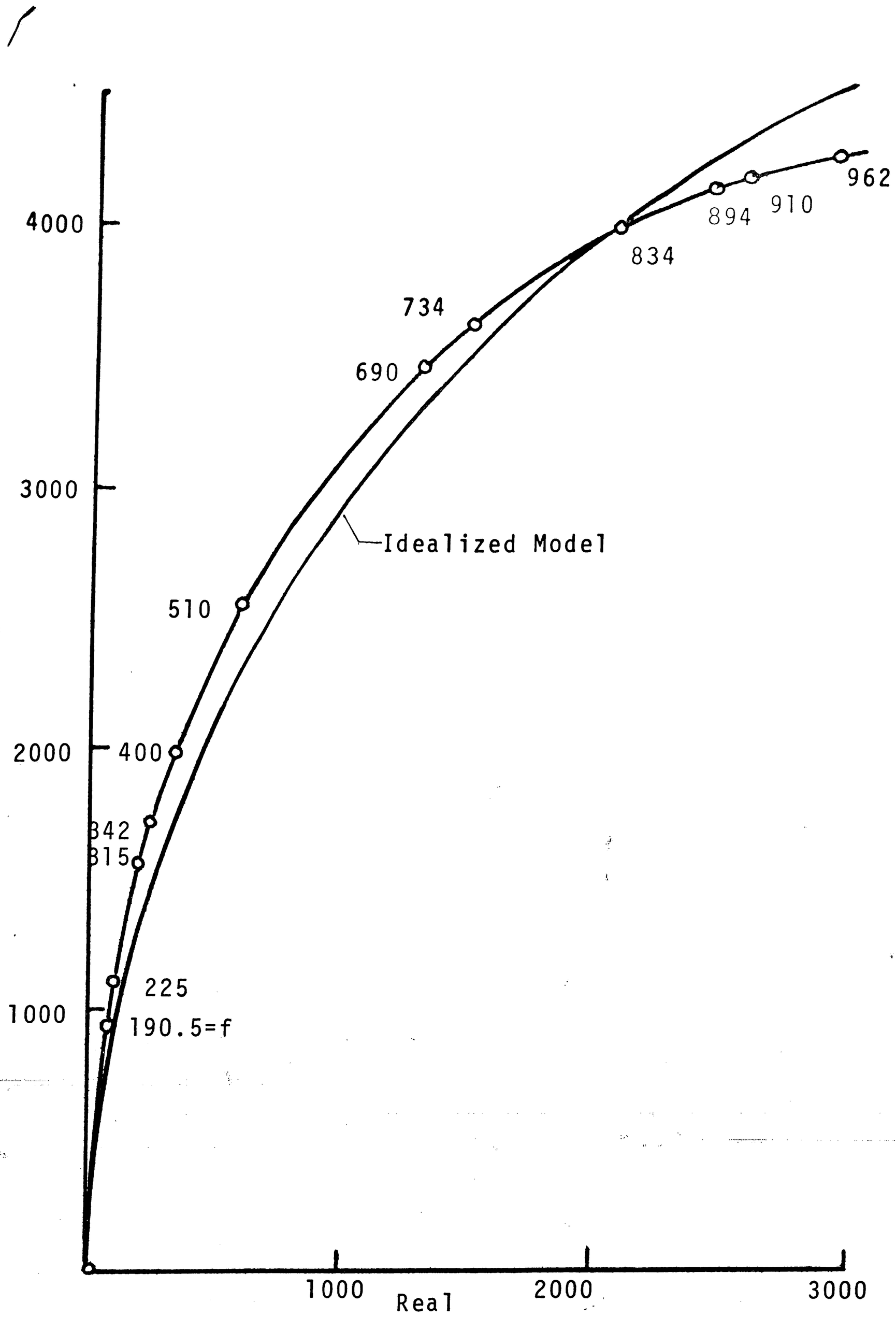

Figure 31. The Product YR_b.

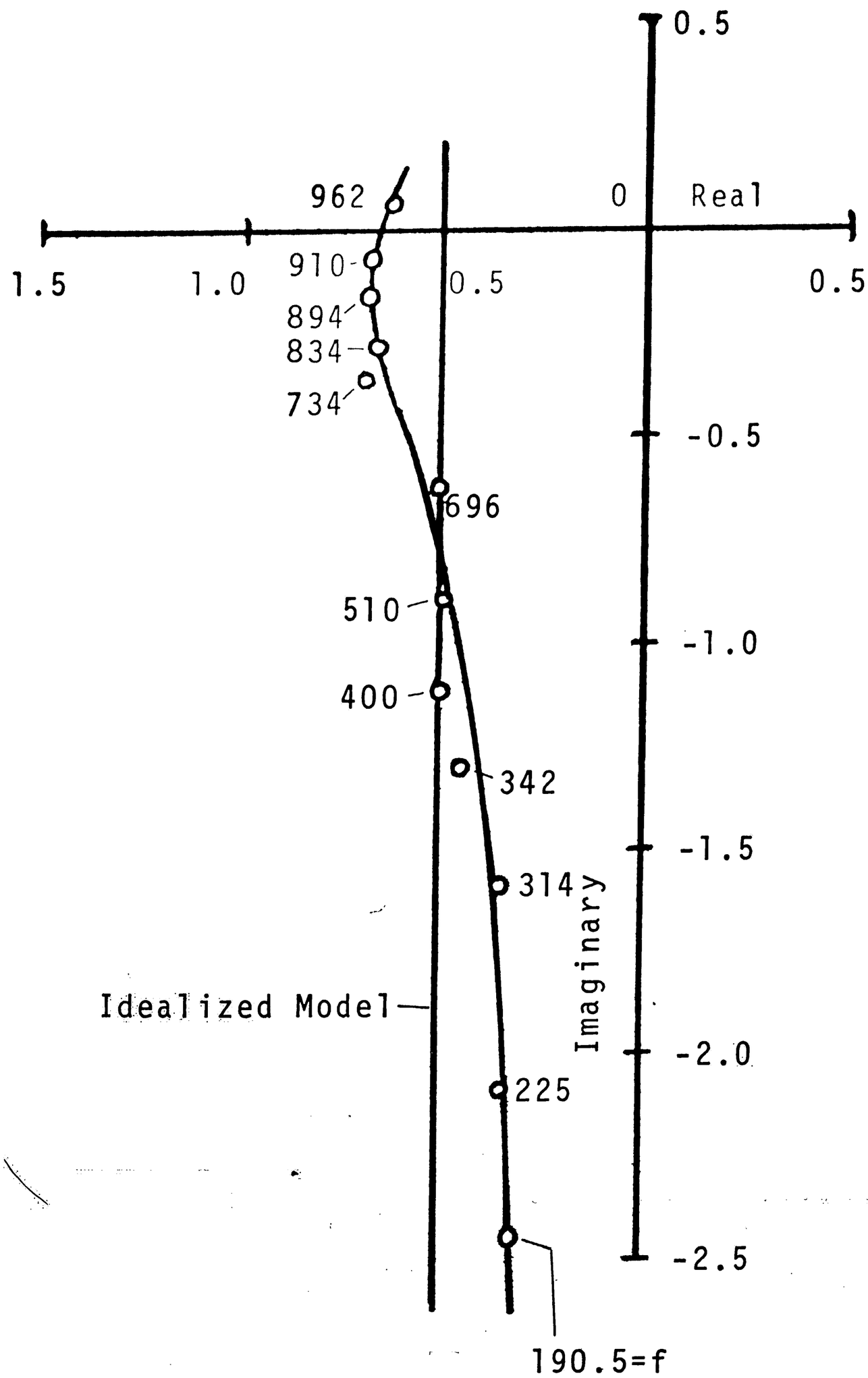

Figure 32. Nyquist Plot of Loop Gain of the Operational Amplifier.

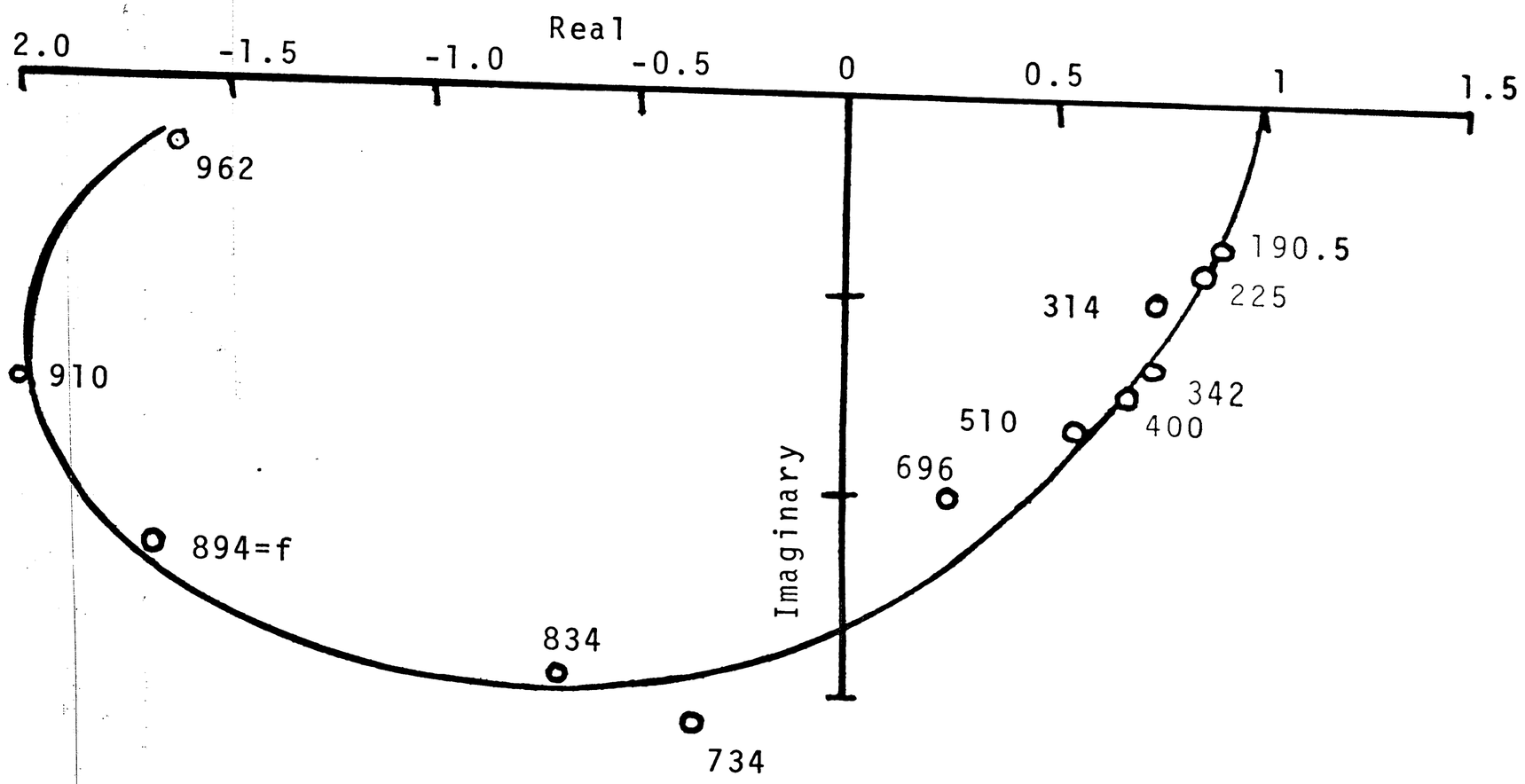

Figure 33. Predicted Closed-Loop Gain of the Operational Amplifier.

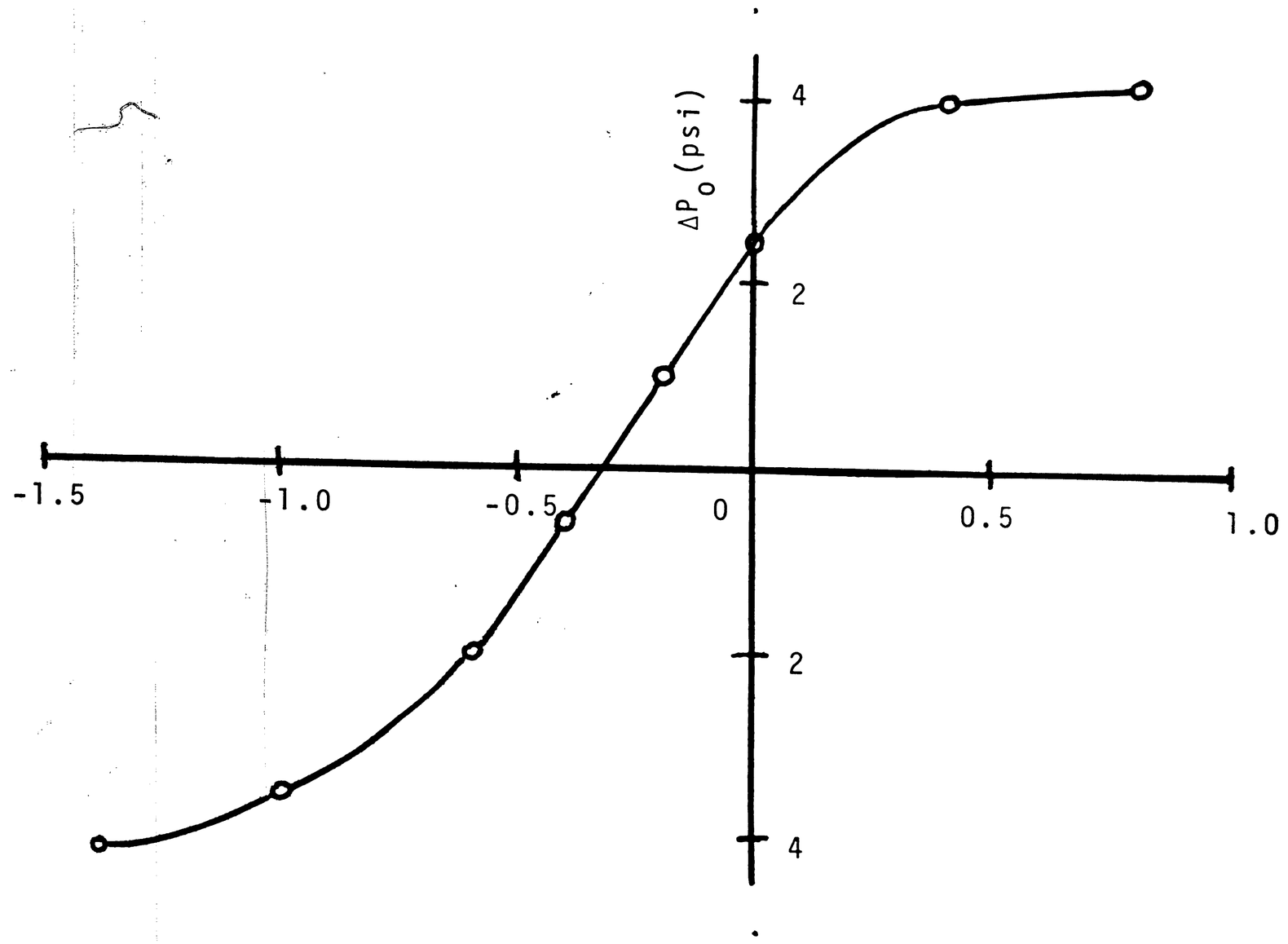

Figure 34. Static Gain Characteristics of Operational Amplifier.

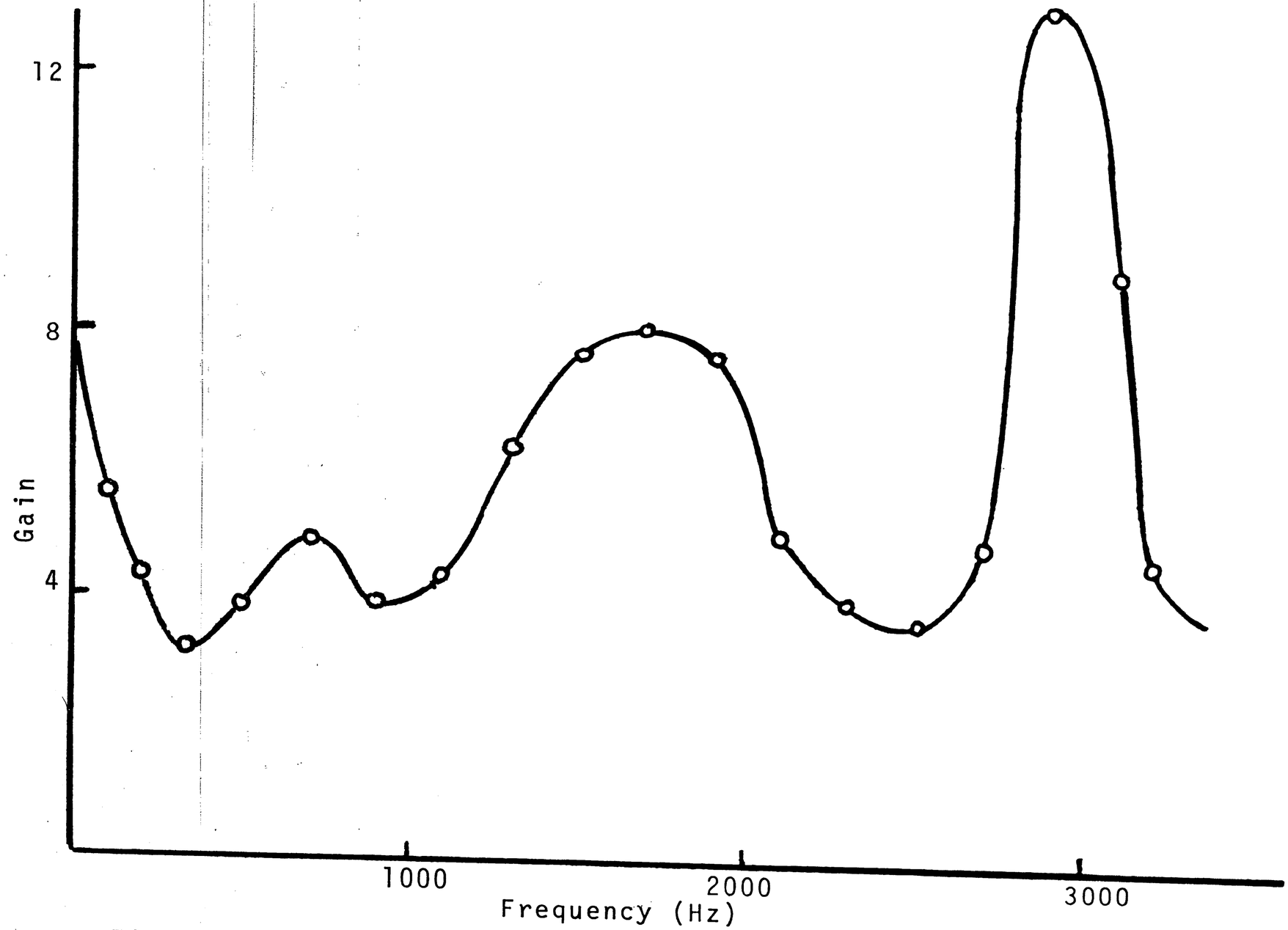

Figure 35. Frequency Response of the Basic Operational Amplifier.

VITA

Tahir Sheikh, son of Siddiq and Tayyaba Sheikh was born on March 17, 1948 in Karachi, Pakistan. He obtained his General Certificate of Education "O" level (University of Cambridge, England) in December 1962 and his Higher Secondary Certificate in August 1964 from the Board of Education, Karachi. He completed his Bachelor of Science in 1966 from the University of Karachi and did his undergraduate studies in Mechanical Engineering at the N. E. D. Government Engineering College, Karachi. He received his B. M. E. degree in November 1970 and joined Lehigh University in February 1971 for his graduate studies.